Title

Integrated Roadway / Adaptive Cruise Control System: Safety, Performance, Environmental and Near Term Deployment Considerations

Authors

Zhang, Jianlong
Ioannou, Petros

Publication Date

2004-09-01

CALIFORNIA PATH PROGRAM
INSTITUTE OF TRANSPORTATION STUDIES
UNIVERSITY OF CALIFORNIA, BERKELEY

Integrated Roadway/Adaptive Cruise Control System: Safety, Performance, Environmental and Near Term Deployment Considerations

Jianlong Zhang, Petros Ioannou
University of Southern California

California PATH Research Report
UCB-ITS-PRR-2004-32

This work was performed as part of the California PATH Program of the University of California, in cooperation with the State of California Business, Transportation, and Housing Agency, Department of Transportation; and the United States Department of Transportation, Federal Highway Administration.

Final Report for Task Order 4242

September 2004

ISSN 1055-1425

Integrated Roadway/Adaptive Cruise Control System: Safety, Performance, Environmental and Near Term Deployment Considerations

Final Report: TO4242

By

Jianlong Zhang

Petros Ioannou

Center for Advanced Transportation Technologies

University of Southern California

EE-Systems, EEB200, MC2562

Los Angeles, CA 90089

July 30, 2004

Abstract

In this project, we design two new Adaptive Cruise Control (ACC) systems based on driver comfort, safety, vehicle following performance, environmental and traffic flow characteristics considerations. A new variable time headway rule is proposed and used to meet these considerations. Analysis and simulations are used to evaluate and compare the two designs. The first ACC system (referred to as ACC01) incorporates two controllers: one for speed tracking and one for vehicle following. The second ACC system (referred to as ACC02) treats the vehicle following task as a special speed tracking task and incorporates more intelligence in dealing with disturbance rejection, smooth response and safe vehicle following without affecting travel time. It provides better transient performance than ACC01, and can attenuate oscillations in the speed response of the preceding vehicle. It has also been shown that ACC02 provides better fuel economy and emission results than ACC01. The ACC02 design will be used for subsequent studies in a continuation project.

Keywords: adaptive cruise control, variable time headway, adaptive control, fuel economy, emission, fundamental flow-density diagram

Executive Summary

This is the Final Report for project under TO4242. In this project, we design two ACC systems, referred to as ACC01 and ACC02 that can be implemented with a general variable time headway that includes those proposed in the literature as well as new ones. The ACC systems are developed based on a simplified longitudinal vehicle model and have been proven to be able to guarantee global stability. Simulations are conducted with a validated nonlinear vehicle model to demonstrate that both ACC systems work in a safe manner and meet the control objectives. The ACC01 has similar properties as the ACC systems proposed in the literature whereas ACC02 is different and is equipped with more intelligence when it comes to disturbance rejection and smooth response. It is observed that under certain conditions the transient response of ACC01 violates the control objective when the preceding vehicle accelerates rapidly. Furthermore, the oscillations in the speed of the preceding vehicle will be propagated back unattenuated by ACC01 even when the separation distance is very large. This is typical of the ACC systems proposed in the literature where in an effort to guarantee tight vehicle following they follow closely oscillatory speed responses of the lead vehicle. ACC02 treats the vehicle following task as a special case of the speed tracking task, and is designed to provide better transient performance by using a nonlinear logic function. As a result the oscillations in the speed response of the preceding vehicle can be efficiently attenuated when the separation distance is large. This special property of ACC02 leads to better fuel economy and emission results than ACC01.

We establish that on the macroscopic level the effect of ACC on traffic flow characteristics depends on the spacing rule used rather than the type of individual control system on board of each vehicle. As a result ACC01 and ACC02 have similar properties on the macroscopic level if both use the same spacing rule. When large constant time headways are used, the presence of ACC vehicles decreases not only the capacity but also the critical density of the traffic flow. We propose and analyze a new variable time headway which is parameterized by a design constant r which is interpreted as the ratio of the time headway used by ACC vehicles versus that of manually driven vehicles. For $r<1$ the presence of ACC vehicles appears to improve the traffic flow characteristics whereas for $r>1$ the traffic flow of mixed traffic becomes unstable at lower traffic densities and at lower traffic flows compared with the traffic with no ACC vehicles.

Our study concludes that the ACC02 with the new proposed variable time headway with $r<1$ provides the best performance with respect to vehicle following, environment and traffic flow characteristics. Safety considerations may require r to be not much less than 1 or additional technologies may be used to improve the reaction time of ACC during braking maneuvers. The ACC02 system is also able to receive speed commands from the roadway and respond in a smooth way without any adverse effect on travel time. ACC02 will be used in a continuing project under TO5501 to develop a roadway controller in an integrated roadway/ACC system which can be implemented in today's highway system.

TABLE OF CONTENTS

LIST OF FIGURES

LIST OF TABLES

1 INTRODUCTION

During the last decade considerable progress has been made in the area of Intelligent Transportation Systems (ITS) both on the research and testing levels [1-6]. Sensor technologies for ITS applications, control and communication protocols, field tests, and experiments in controlled environments have been carried out. While dedicated highways with fully automated vehicles is a far in the future objective [7], the introduction of semi-automated vehicles, such as vehicles with Adaptive Cruise Control (ACC), also referred to as Intelligent Cruise Control (ICC), on current highways designed to operate with manually driven vehicles has already taken place in Japan and Europe and more recently in the US too [8]. This technology allows the ACC vehicle to follow a preceding vehicle automatically by maintaining a chosen by the driver inter-vehicle spacing. Due to liability and safety issues the ACC systems deployed are rather conservative and rely on the driver for hard braking and emergencies.

These initial ACC systems are designed for driver comfort under rather conservative safety constraints and are often marketed as driver assist devices. No consideration was given to the effect of ACC systems on traffic flow characteristics and environment beyond the obvious string stability issue. It has been argued that some versions of the ACC deployed could actually have a negative effect on traffic flow and possibly on the environment while other versions could help smooth traffic flow and in certain situations attenuate and contribute to a faster dissipation of shock waves and therefore have beneficial effects on the environment. It has been shown that the presence of 10% ACC vehicles in the highway traffic lowers the fuel consumption and pollution levels by as much as 8% and 3.8% to 47.3% respectively during traffic disturbance scenarios [9]. The impact of advanced transportation systems on the environment and traffic flow characteristics attracted the interest of several researchers. In [10] the potential impact of Advanced Public Transportation Systems (APTS) on air quality and fuel economy was studied and concluded that transit buses produce less hydrocarbon (HC) and carbon monoxide (CO) emissions than autos on a passenger-mile basis. In [11] different Intelligent Transportation Technologies (ITS) have been discussed that have the potential to improve air quality, including reduction of unnecessary “stop and go” type of traffic. In Ioannou and Chien [1, 12] estimates of the capacity improvement due to ACC are obtained for different vehicle following concepts where different minimum time headways are used based on safety considerations. The results show that if time headways employed by the ACC vehicles are smaller than those used by the average driver, the penetration of ACC vehicles is expected to improve capacity otherwise larger time headways employed by the ACC vehicles for higher safety tolerances may reduce capacity and in addition invite cut ins. In [13] a micro simulator referred to as the SPEACS and the fundamental diagram were used to study the effect of ACC on traffic flow in a mixed traffic environment. The ACC vehicles were assumed to have time headways of 1 second and 2 seconds in two different simulations that involved a two-lane highway system 6 Km long. They concluded that with time headways of 1 second the maximum traffic flow rate sustained was improved by 6% and 13% for 20% and 40% ACC vehicle penetration respectively. On the other hand ACC vehicles with 2-seconds

time headways reduced the maximum traffic flow rate by 3% and 6% for 20% and 40% ACC vehicle penetration respectively. Minderhoud and Bovy [14] tested several ACC operating concepts with time headways varying from 1 to 1.4 seconds. The results show that small time headways will increase capacity as the ACC penetration increases whereas headways greater than 1.2 sec will decrease capacity. Vanderwerf et al [15] at PATH used Monte Carlo simulations to evaluate the effects of ACC and the so-called Cooperative ACC (CACC) in mixed traffic using a human driver model developed in [16]. The CACC is referred to ACC systems involving vehicle-to-vehicle communication [13, 17] for exchanging information regarding deceleration characteristics and maneuvers between lead and following vehicle. The simulations in [15] demonstrated that the use of time headways of 1.4 seconds an average of what current ACC systems are allowed to use will lead to small increases in capacity at penetrations up to 60% whereas for penetrations above 60% a loss of capacity was observed. Van Arem et al [18] used a simulation model referred to as MIXIC to study the effects of ACC on traffic flow characteristics using time headways of 1 and 1.5 seconds. They demonstrated that ACC systems contribute to a more stable flow, however as the demand increases the traffic flow performance begins to deteriorate. This observation is consistent with the analysis performed by Swaroop et al [19] and confirmed by Bose et al [20] using the fundamental diagram that with ACC vehicles the operating point corresponding to maximum traffic flow rate is unstable or rather more unstable than manually driven vehicles.

It has been noticed that using variable time headways may lead to better traffic or vehicle following performance. In [21], Swaroop et al attempted to use traffic flow considerations to come up with time headway based on the hypothesis proposed by Greenshields [22]. In this case, the time headway is a strictly decreasing function of the traffic density, or equivalently, a strictly increasing function of the ACC vehicle's speed. They demonstrated via simulations that the new spacing policy has a better effect on traffic flow than the constant time headway policy. In [23], a variable time headway was proposed for tightly vehicle following control, which depends on the speeds of the ACC vehicle and its preceding vehicle. The simulation results demonstrated that the vehicle following performance is improved using such a time headway. Other implementations of variable time headways can be found in [24, 25]. The design and analysis of ACC systems in the current literature is performed based on safety, driver comfort and vehicle following performance considerations. While ACC are analyzed or simulated for traffic flow characteristics and impact on environment in addition to vehicle following performance no attempts are made to design ACC systems by taking all relevant considerations into account.

The objectives of this project were to design ACC systems based on safety, driver comfort, vehicle following performance as well as on environmental and traffic flow characteristic considerations and evaluate them using analysis and simulations. Such ACC systems would be designed to operate in an integrated roadway/ACC system to be completed in a continuation project of TO4242. In this project these objectives have been met as described below. We start by designing two ACC systems employing different variable time headways that include those in [21-25] as well as constant time headway. We show that the first one (ACC01) has desired stability properties and can meet the

control objectives when following a preceding vehicle with a constant speed. However, its transient performance cannot be always guaranteed when the preceding vehicle accelerates rapidly or it has an oscillatory speed response. The second one (ACC02), on the other hand, is designed to reject disturbances and smooth possible oscillations in the speed response of the preceding vehicle, and demonstrated via simulations to have better transient performance. The simulation results are also used to demonstrate that ACC02 can provide better fuel economy and emission results than ACC01 due to its smoother response and disturbance rejection properties. The behavior of ACC vehicles in mixed traffic on the macroscopic level is analyzed. Two time headways are considered here, one is the constant time headway and the other is the variable one based on the Greenshields relationship. For constant time headway, it is found out that for relatively small time headways the presence of ACC vehicles appears to improve traffic flow characteristics whereas for large time headways the traffic flow of mixed traffic becomes unstable at lower traffic densities and at lower traffic flows compared with traffic with no ACC vehicles. In the case of variable time headway, the effect of ACC vehicles on traffic flow characteristics depends on r, the ratio of the time headway used by ACC vehicles versus that of manually driven vehicles. For $r<1$ the presence of ACC vehicles appears to improve the traffic flow characteristics whereas for $r>1$ the traffic flow of mixed traffic becomes unstable at lower traffic densities and at lower traffic flows compared with traffic with no ACC vehicles.

The report is organized as follows: In section 2 we design and analyze two ACC systems and simulations are conducted to demonstrate and compare their performance. In section 3 we compare the environmental performance of the two ACC systems using the simulation results in section 2. In section 4 fundamental flow-density diagrams are used to investigate the impacts of ACC vehicles on mixed traffic flow. The conclusions are presented in section 5.

2 ADAPTIVE CRUISE CONTROL DESIGN

The Adaptive Cruise Control (ACC) system is an extension of the conventional Cruise Control (CC) system. In addition to the autonomous speed regulation provided by the conventional CC systems, the ACC system provides the intelligent function that enables the ACC vehicle to adjust its speed automatically in order to maintain a desired intervehicle spacing between itself and a moving preceding vehicle or obstacle in the same lane. When the lane is clear, i.e. no object is detected by the forward-looking sensor installed on the vehicle, the ACC system works in the speed tracking mode and regulates the vehicle speed towards the desired speed set by the driver or a roadway controller (in the case of a future advanced traffic system). Otherwise, the ACC system works in the vehicle following mode and regulates the vehicle speed to maintain a desired spacing from the vehicle or obstacle ahead. In the ACC design, lateral control is the responsibility of the driver and driving in the ACC mode involves lanes with small curvatures. Therefore the lateral dynamics are considered to be decoupled from the longitudinal dynamics. In this report, we refer to the longitudinal vehicle model as the vehicle model.

2.1 Simplified Vehicle Model for Control Design

The vehicle model used for simulations is taken from [26]. It was built based on physical laws and had been experimentally validated. This model can be characterized by a set of differential equations, algebraic relations and look-up tables. This validated model is very complex but can be viewed as a first-order nonlinear system [26]

$$\dot{v} = f(v, u, t) \tag{2-1}$$

where v is the longitudinal speed, u is the throttle/brake command and t represents the negligible fast dynamics. The complete vehicle model in (2-1) is highly nonlinear, thus not suitable for control design. In our work, the simple first-order model

$$\dot{v} = -a(v - v_d) + b(u - u_d) + d \tag{2-2}$$

where v_d is the desired steady state speed, u_d is the corresponding steady state fuel command, d is the modeling uncertainty, and a and b are constant parameters that depend on the operating point, i.e. the steady state values of the vehicle speed and load torque is used for ACC design [23, 26]. If there is no shift of gears, a and b are positive. In our analysis, we assume that a and b are always positive since any gear shift results in a short time transient activity. For a given vehicle, the relation between v_d and u_d can be described by a look-up table, or by a 1-1 mapping continuous function

$$v_d = f_u(u_d) \tag{2-3}$$

In our analysis, we assume $f_u(u_d)$ is differentiable and

$$m_u \le \frac{d}{du_d} f_u(u_d) \le M_u \tag{2-4}$$

where m_u and M_u are two positive constants. The simplified vehicle model used for ACC design is described by (2-2) - (2-4). We assume that $d, \dot{d}$ v_l and $\dot{v}_l$ are all bounded and continuous.

2.2 Control Objectives and Constraints

In the speed tracking mode, the ACC system regulates the vehicle speed v close to the desired speed v_d set by the driver or by the roadway controller in an advanced vehicle highway system [27]. The control objective can be expressed as

$$\lim_{t\to\infty} e_v(t) = 0 \tag{2-5}$$

where $e_v(t) = v_d(t) - v(t)$.

In the vehicle following mode, the ACC system regulates the vehicle speed so that it follows the preceding vehicle by maintaining a desired intervehicle spacing. The control objective is to regulate the vehicle speed v to track the speed of the preceding vehicle v_l while maintaining the intervehicle spacing x_r as close to the desired spacing s_d as possible, as shown in Figure 1. With the time headway policy, the desired intervehicle spacing is given by

$$s_d = s_0 + hv \tag{2-6}$$

where s_0 is a fixed safety intervehicle spacing to avoid vehicle contact at low or zero speeds and h is the time headway. The control objective in the vehicle following mode can be expressed as

$$v_r \to 0, d \to 0 \text{ as } t \to \infty \tag{2-7}$$

where $v_r = v_l - v$ is the speed error and $d = x_r - s_d$ is the separation error. In practice, this control objective may not be met exactly when v_l varies considerably, or in the presence of sensor noise, modeling errors, delays and other imperfections. For safety reasons the time headway should be chosen large enough and the ACC system should be designed to be robust with respect to these imperfections so that d remains non-negative most of the time, i.e. the ACC vehicle follows the preceding vehicle in a safe manner.

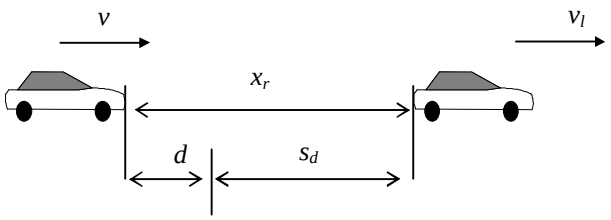

Figure 1. Diagram of the vehicle following mode

Even though the ACC system has two different control objectives in the speed tracking and vehicle following modes, the following control constraints have to be satisfied in both modes [26]:

C1. $a_{\min} \leq \dot{v} \leq a_{\max}$ where $a_{\min}$ and $a_{\max}$ are specified.
C2. The absolute value of jerk defined as $|\ddot{v}|$ should be small.

The above constraints are the result of driving comfort and safety concerns and are established using human factor considerations [26].

2.3 Variable Time Headway

In our work, we consider the time headway as a function of v and v_l, i.e. $h(v, v_l)$, which has bounded partial derivatives with respect to v and v_l. Most of the previous studies for vehicle following control considered constant spacing rules (h=0) and constant time headway spacing rule (h = nonzero constant). In some recent studies it has been suggested that a variable time headway in the ACC system may lead to better performance in terms of safety and traffic flow. In [24], the desired spacing is chosen as

$$s_d = s_0 + h_1 v + h_2 v^2 \tag{2-8}$$

where h_1 and h_2 are two positive constants. The time headway incorporated in (2-8) depends on the speed of the following vehicle, which can be expressed as

$$h = h_1 + h_2 v \tag{2-9}$$

In [21, 28], the time headway is chosen based on the hypothesis proposed by Greenshields [22], and it can be written as

$$h = \frac{1}{k_{jam}\left(v_{free} - v\right)} \tag{2-10}$$

where k_{jam} is the traffic density corresponding to a maximum congestion condition and v_{free} is the free speed when the traffic density is low. Note that the time headway in (2-10) is expressed in a different way than that in [28] because the spacing considered in [28] incorporates the vehicle length.

In [23], the time headway h proposed for tightly vehicle following control is given as

$$h = sat(h_0 - c_h v_r) \tag{2-11}$$

where h_0 and c_h are positive constants to be designed and the saturation function $sat(\bullet)$ has an upper bound 1 and a lower bound 0. Even though this nonlinear time headway associated with proper vehicle following controllers leads to desired platoon performance as demonstrated in [23], no global stability properties have been established for the closed loop simplified vehicle model. Let us define

$$H = \frac{\partial}{\partial v} s_d(v, v_l) \tag{2-12a}$$

$$H_l \cong \frac{\partial}{\partial v_l} s_d(v, v_l) \tag{2-12b}$$

For the constant time headway spacing rule, H is equal to the time headway h and H_l is zero. All the time headway rules mentioned above share the property that $H \geq 0$, and this property will be taken into account for the vehicle following control design. As we mention above, we assume that H and H_l are bounded. Apparently, the time headway given in (2-9) is unbounded if v is unbounded. However, in practice it is impossible to employ time headways involving arbitrarily large H and H_l. We therefore modify the time headway as

$$h = \begin{cases} h_1 + h_2 v, & \text{if } v < v_{\max} \\ h_1 + h_2 v_{\max}, & \text{otherwise} \end{cases} \tag{2-13}$$

where $v_{\max}$ is the maximum speed the following vehicle can achieve. This modified time headway guarantees H and H_l are bounded. Similarly, we can also modify the time headway given in (2-10) so that H and H_l are bounded.

It should be noted that the time headway used in the ACC systems should never violate the safety constraint. Extensive studies have been done to investigate safety spacing based on different braking emergency scenarios [29]. However, [29] only considers the minimum constant time headway that should be kept to guarantee safety for all speeds. In our discussion, the assumptions in [29] are used but the investigation is not restricted to the minimum constant time headway. This leads to the situation in which the time headway could be chosen as a function of the vehicle speed. Similar results can be

found in other publications, such as [30], with different assumptions. In this subsection, we use the notation of v_f for the speed of ACC vehicle.

Consider the braking situation shown in Figure 2 [29]. The initial speeds of the lead and following vehicles are $v_l(0)$ and $v_f(0)$, respectively. At time zero, the following vehicle accelerates with a_{fac}, while the lead vehicle performs emergency braking with its maximum jerk J_{lm} until it reaches its maximum deceleration a_{lm}. This maximum deceleration is kept until the speed of the lead vehicle becomes zero. After a certain delay (t_1), the following vehicle detects the braking maneuver of the lead vehicle, and it starts to brake after some reaction time (t_2). Since it is not known whether the vehicle ahead is just adjusting its speed or executing an emergency braking, the following vehicle starts to brake with certain jerk (J_{fc}) at time t_{fa}, reaches deceleration rate a_{fauto} at time t_{fb}, and keeps this deceleration rate for some time (t_3) until at time t_{fc} it realizes the vehicle ahead is doing an emergency braking. Then the following vehicle begins hard braking with the maximum rate of J_{fm} until the maximum deceleration a_{fm} is achieved.

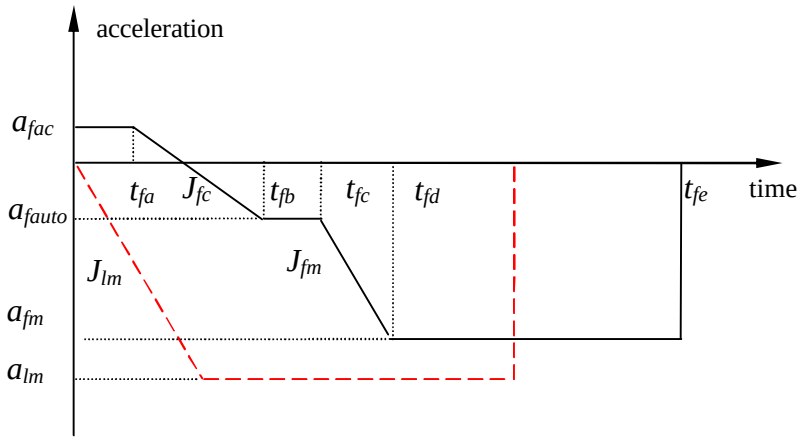

Figure 2. Acceleration trajectories of two vehicles in the worst braking scenario.

Since we consider a worst case braking situation, it is reasonable to assume that $v_l(0) \le v_f(0)$, $|J_{lm}| \ge |J_{fm}|$ and $|a_{lm}| \ge |a_{fm}|$. Hence the speed of the following vehicle is always higher or equal to that of the lead one. In this case, the minimum spacing $S_{\min}$ that guarantees no collision is given by

$$S_{\min} = s_0^* + a_l v_l(0) + a_f v_f(0) + b_l v_l^2(0) + b_f v_f^2(0) \qquad (2\text{-}14)$$

where $b_l = 1/(2a_{lm})$, $b_f = -1/(2a_{fm})$, $a_l = -a_{lm}/(2J_{lm})$, and a_f and s_0^* are relatively complex functions of the parameters associated with the following vehicle's deceleration trajectory. For tight vehicle following, we can assume $v_l(0) = v_f(0) = V$, and then the minimum separation can be expressed as

$$S_{\min} = s_0^* + h_1^* V + h_2^* V^2 \qquad (2\text{-}15)$$

where $h_1^* = a_l + a_f$ and $h_2^* = b_l + b_f$. To get a better understanding of (2-15), we further assume that J_{lm}, J_{fm} and J_{fc} are very large, and a_{fac} and a_{fauto} are very small. Hence

$$s_0^* \approx 0 \tag{2-16a}$$

$$h_1^* \approx t_1 + t_2 + t_3 \tag{2-16b}$$

$$h_2^* = \frac{1}{2}\left(\frac{1}{a_{lm}} - \frac{1}{a_{fm}}\right) \tag{2-16c}$$

Here we can see that h_1^* depends mostly on the delays in the sensing, control and actuation systems, but h_2^* depends only on the maximum deceleration capacity of the following vehicle. The minimum safety spacing for a given vehicle should be calculated with the assumption that the lead vehicle has the maximum braking capacity. If the following vehicle also has the maximum capacity, i.e. $a_{lm} = a_{fm}$, then $h_2^* = 0$. However, $a_{lm} = a_{fm}$ may not be a reasonable assumption since different types of vehicles have different braking capacities. For a heavy-duty vehicle with full load, h_2^* could be a large number. Consider the parameters given in Table 1. These values are taken from [29]. The minimum safety spacing based on these values is calculated as

$$S_{\min} = 0.01 + 0.363V + 0.011V^2 \tag{2-17}$$

This minimum safety spacing has been assumed in the simulation studies in this report.

$v_l(0)$	26.8m/s (60mph)		a_{fm}	-7.5m/s^2 (-0.77g)
$v_f(0)$	26.8m/s (60mph)		a_{fauto}	-1.96m/s^2 (-0.2g)
J_{lm}	-72m/s^3		a_{fac}	0.49m/s^2 (0.05g)
J_{fm}	-72m/s^3		t_1	0.1s
J_{fc}	-20m/s^3		t_2	0.1s
a_{lm}	-9.1m/s^2 (-0.93g)		t_3	0.1s

Table 1. Parameter values for safety spacing calculation

2.4 ACC Design Strategy 1

2.4.1 Control Design for Speed Tracking

Based on the simplified vehicle model, different design methodologies can be applied for speed tracking control. It has been shown that a PID controller meets the control objectives for speed tracking [31]. We adopt this controller in our work since it is very simple and can be easily implemented.

Lemma 2.1[31]: For the system represented in (2-2) - (2-4), the following PID controller

$$u = k_p e_v + k_i \frac{1}{s} e_v + k_d \frac{s}{\frac{1}{N}s + 1} e_v \tag{2-18}$$

where k_p, k_i, k_d and N are some positive parameters, can stabilize the closed-loop system and guarantee that $e_v(t)$ converges exponentially fast to the residual set

$$E_v = \left\{ e_v \in R \middle| |e_v| \le C_1 \cdot \left\| \dot{v}_d(t) \right\|_\infty + C_2 \cdot \left\| \dot{d}(t) \right\|_\infty \right\} \tag{2-19}$$

where C_1 and C_2 are some positive constants. Furthermore, if v_d and d are constants, then $e_v(t)$ converges to zero exponentially fast.

ÿ

Since the desired speed v_d set by the driver or the roadway controller may vary, the initial speed tracking error may be large leading to a large control effort and high acceleration which may violate the constraints given above. To avoid such situations, we use the same nonlinear filter (shown in Figure 3) employed in [31] to generate a smooth reference signal v_{ref}, and force the vehicle to track the modified smoother signal v_{ref}. In this nonlinear filter, p is a positive constant, and the saturation function is used to limit the varying rate of v_{ref}. The upper and lower bounds of the saturation function, $a_{\max}$ and $a_{\min}$, are chosen in a way the driver feels comfortable and unsafe situations are avoided when v tightly tracks v_{ref}. This nonlinear filter was first used in [26] for the design of vehicle following controllers, and then adopted in [31] for speed tracking control. If v_d is a constant, then $\lim_{t\to\infty} v_{ref}(t) = v_d$ and the control objective in (2-5) can still be achieved when d in (2-2) is also a constant.

A simple switching logic is adopted from [31] to avoid frequent chattering between the brake and throttle subsystems. According to (2-6), a fuel command is issued when u is positive, while the brake is activated when $u<-u_0$ ($u_0>0$ is a constant). If $-u_0 \le u \le 0$, the brake system is inactive and the throttle is operating as in idle speed.

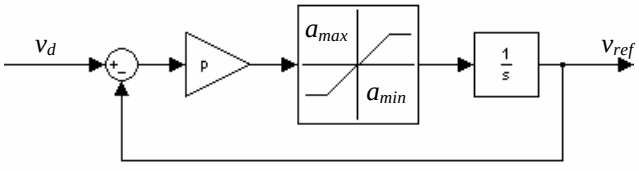

Figure 3. Nonlinear filter used in the speed tracking mode

2.4.2 Control Design for Vehicle Following

The simplified longitudinal model described by (2-2) - (2-4) is used for the vehicle following control design. In this design, the desired steady state speed v_d is equal to v_l, the speed of the lead vehicle. In [21], a vehicle following controller using the variable time headway in (2-10) was proposed based on feedback linearization. The desired closed-loop system is described by

$$\dot{d} = -kd \tag{2-20}$$

where k is a positive constant. If all the parameters in the simplified model are known, the vehicle following controller

$$u = \frac{1}{bH}(v_r + kd) - \frac{a}{b}v_r + \left(u_d - \frac{d}{b} - \frac{H_l}{bH}\dot{v}_l\right) \tag{2-21}$$

can be used. The control design procedure is straightforward, but the controller in (2-21) has some obvious flaws. It is a high gain controller when H is small, which may not be desired. Furthermore, this controller cannot be implemented when H is equal to zero. Obviously H is zero in the constant spacing rule and may also be zero when the nonlinear time headway given in (2-11) is used. The vehicle following controllers proposed in this section guarantee global stability for any variable time headway that has bounded H and H_l with $H \geq 0$.

One important issue associated with vehicle following control is string stability. String stability in a vehicle string implies that any nonzero speed and separation error of an individual vehicle does not get amplified as it propagates upstream [32, 33]. Here we consider only L_2 string stability [33]. In the string stability analysis, we assume that the lead vehicle slowly varies its speed around the nominal value v_{l0}, and the vehicle following controller can sufficiently keep v_r and d close to zero.

Lemma 2.2: Consider the system (2-2) - (2-4), with the following controller

$$u = k_1^* v_r + k_2^* \Delta(d, t) + k_3^* \tag{2-22}$$

where $k_1^* = \frac{a_m - a}{b}$, $k_2^* = \frac{a_m}{b}$, $k_3^* = u_d - \frac{d}{b}$, Δ is a design time varying function of d satisfying

$$k_l d \leq \Delta(d, t) \leq k_u d \tag{2-23}$$

and a_m, k_l and k_u are positive design constants.
(i) All the signals in the closed-loop system are bounded if a_m, k_l and k_u are designed such that there exists a positive constant p_1 satisfying

$$a_m p_1 > 1 \tag{2-24a}$$

$$a_m p_1^2 (k_u - k_l)^2 - 4k_u (a_m p_1 - 1) < 0 \tag{2-24b}$$

$$a_m + a_m k_l p_1 - k_u \geq 0 \tag{2-24c}$$

$$\frac{4 p_1 k_l}{a_m + a_m k_l p_1 - k_l} > \sup H \tag{2-24d}$$

where sup$H$ is the supremum of H. Furthermore, if v_l is a constant, then the control objective in (2-7) is achieved, i.e. $v_r, d \to 0$ as $t \to \infty$.

(ii) If Δ is a time invariant and differentiable function of d, then local L_2 string stability is guaranteed provided the control parameters are chosen such that

$$a_m \Delta_d (0)\left(H^2 - H_l^2\right) + 2a_m (H + H_l) - 2 \geq 0 \tag{2-25}$$

where $\Delta_d = \partial\Delta / \partial d$.

Proof: Let $\Delta(d, t) = kd$ where k is a time varying function of d and satisfies $k_l \leq k \leq k_u$. Using (2-22) in (2-2)-(2-4), the closed-loop system is

$$\dot{v} = a_m (v_r + kd) \tag{2-26}$$

(i) Denote $x_1 = v_r$ and $x_2 = d$, then

$$\begin{cases} \dot{x}_1 = -a_m (x_1 + k x_2) + u_1 \\ \dot{x}_2 = (1 - a_m H) x_1 - a_m k H x_2 - H_l u_1 \end{cases} \tag{2-27}$$

where $u_1 = \dot{v}_l$, H and H_l are bounded with $H \geq 0$ (recall the assumptions in section 2.3). Consider the following candidate Lyapunov function

$$V_a = \tfrac{1}{2} x^T P x \tag{2-28}$$

where $P = \begin{bmatrix} p_1 & 1 \\ 1 & p_2 \end{bmatrix}$ a positive definite matrix, and p1 and p2 is are positive constants. Hence,

$$
\begin{aligned}
&\dot{V}_a = p_1 x_1 \dot{x}_1 + p_2 x_2 \dot{x}_2 + x_1 \dot{x}_2 + \dot{x}_1 x_2 \\
&= p_1 x_1 \left[- a_m \left(x_1 + k x_2 \right) + u_1 \right] + p_2 x_2 \left[\left(1 - a_m H \right) x_1 - a_m k H x_2 - H_l u_1 \right] \\
&+ x_1 \left[\left(1 - a_m H \right) x_1 - a_m k H x_2 - H_l u_1 \right] + x_2 \left[- a_m \left(x_1 + k x_2 \right) + u_1 \right] \\
&= - x_1^2 \left(a_m p_1 - 1 + a_m H \right) - x_2^2 \left(a_m k + a_m k H p_2 \right) \\
&- x_1 x_2 \left(a_m k p_1 + a_m - p_2 + a_m H p_2 + a_m k H \right) \\
&+ u_1 \left(p_1 x_1 - H_l x_1 + x_2 - H_l p_2 x_2 \right)
\end{aligned}
\tag{2-29}
$$

We choose

$$
p_2 = a_m k_l p_1 + a_m \tag{2-30}
$$

When (2-24a) holds, the coefficient of x_1^2 in (2-29) is negative and (2-30) guarantees that P is positive definite. With (2-29), (2-30) can be rewritten as

$$
\begin{aligned}
&\dot{V}_a = - x_1^2 \left(a_m p_1 - 1 + a_m H \right) - x_2^2 \left[a_m k + a_m^2 k H \left(k_l p_1 + 1 \right) \right] \\
&- x_1 x_2 \left(a_m k p_1 - a_m k_l p_1 + a_m^2 H + a_m^2 k_l H p_1 + a_m k H \right) + u_1 \left(w_1 x_1 + w_2 x_2 \right)
\end{aligned}
\tag{2-31}
$$

where $w_1 = p_1 - H_l$ and $w_2 = 1 - H_l (a_m k_l p_1 + a_m)$. Suppose u_1 is zero. Then $\dot{V}_a$ is negative definite if and only if

$$
\begin{aligned}
&\left(a_m k p_1 - a_m k_l p_1 + a_m^2 H + a_m^2 k_l H p_1 + a_m k H \right)^2 \\
&< 4 \left(a_m p_1 - 1 + a_m H \right) \left[a_m k + a_m^2 k H \left(k_l p_1 + 1 \right) \right] \\
&\Leftrightarrow a_m \left[\left(k - k_l \right) p_1 + \left(a_m + a_m k_l p_1 + k \right) H \right]^2 \\
&< 4k \left(a_m p_1 - 1 + a_m H \right) \left[1 + a_m H \left(k_l p_1 + 1 \right) \right] \\
&\Leftrightarrow a_m \left(a_m + a_m k_l p_1 - k \right)^2 H^2 + 2 a_m p_1 \left(k + k_l \right) \left(a_m + a_m k_l p_1 - k \right) H \\
&+ a_m p_1^2 \left(k - k_l \right)^2 - 4k \left(a_m p_1 - 1 \right) < 0
\end{aligned}
\tag{2-32}
$$

One necessary condition for (2-32) to be true is that

$$
a_m p_1^2 \left(k - k_l \right)^2 - 4k \left(a_m p_1 - 1 \right) < 0 \tag{2-33}
$$

for all $k \in [k_l, k_u]$. This condition is equivalent to that (2-24b) is true. When (2-24a) and (2-24b) hold, one sufficient condition for (2-33) to hold is that (2-24c) and (2-24d) hold. Now we have shown that if (2-24a) - (2-24d) hold and u_1 is zero then $\dot{V}_a$ is negative definite. Since w_1 and w_2 are bounded, it is easy to show that V_a is bounded, and then all the signals in the closed-loop system are bounded. Furthermore, if v_l is a constant, i.e. u_1 is zero, it can be verified that $x_1, x_2 \in L_2 \cap L_\infty$, $\dot{x}_1, \dot{x}_2 \in L_\infty$. It follows from Barbalat's Lemma [34] that $x_1, x_2 \to 0$ as $t \to \infty$, i.e., the control objective in (2-9) is achieved.

(ii) With linearization of (2-26), the transfer function from v_l to v is given as

$$G_v(s) = \frac{v}{v_l} = \frac{(a_m - a_m\Delta_d(0)H_l(v_{l0}))s + a_m\Delta_d(0)}{s^2 + [a_m\Delta_d(0)H(v_{l0}) + a_m]s + a_m\Delta_d(0)} \tag{2-34}$$

If we assume all the vehicles in the same lane are of the same type and equipped with the same controller, the vehicle string is L_2 string stable [33] if and only if

$$|G_v(jw)| \le 1, \forall w \ge 0 \tag{2-35}$$

which is equivalent to (2-25).

ÿ

The controller in (2-22) cannot be implemented because *a*, *b* and *d* are unknown parameters which may change with vehicle speed and other conditions. However, we can estimate k_i^* (i=1,2,3) on-line and use their estimate k_i in the control law. In the next Lemma, we show that with proper update laws for k_i, the control law (2-18) where the k_i^* (i=1,2,3) are replaced with their on line estimates meets the control objective.

Lemma 2.3: Consider the system (2-2) - (2-4), with the control law

$$u = k_1 v_r + k_2\Delta(d,t) + k_3 \tag{2-36}$$

where k_i is the estimate of k_i^* (defined in Lemma 2.2) with initial condition k_{i0} (i=1,2,3), generated by the adaptive laws

$$\begin{cases} \dot{k}_1 = \text{Proj}\{g_1 x_1[(p_1x_1 + x_2) + (x_1 + a_m k_l p_1 x_2 + a_m x_2)H]\} \\ \dot{k}_2 = \text{Proj}\{g_2 k x_2[(p_1x_1 + x_2) + (x_1 + a_m k_l p_1 x_2 + a_m x_2)]\} \\ \dot{k}_3 = \text{Proj}\{g_3[(p_1x_1 + x_2) + (x_1 + a_m k_l p_1 x_2 + a_m x_2)H]\} \end{cases} \tag{2-37}$$

where a_m, p_1, g_1, g_2 and g_3 are positive design parameters, Proj{•} is the projection function keeping k_i within the intervals $[k_{il}, k_{iu}]$ (i=1,2,3). k_{il} and k_{iu} are chosen such that $k_i^* \in [k_{il}, k_{iu}]$. If we choose the parameters a_m, k_l, k_u and p_1 such that (2-24a) - (2-24d) hold, i.e.

$$a_m p_1 > 1$$
$$a_m p_1^2 (k_u - k_l)^2 - 4k_u(a_m p_1 - 1) < 0$$
$$a_m + a_m k_l p_1 - k_u \ge 0$$
$$\frac{4p_1 k_l}{a_m + a_m k_l p_1 - k_l} > \sup H$$

then all the signals in the closed-loop system are bounded. Furthermore, if v_l and d are constants, then the control objective in (2-7) is achieved, i.e. $v_r, d \to 0$ as $t \to \infty$.

Proof: With the proposed control law, the closed-loop system becomes

$$\dot{v} = a_m\left(v_r + kd\right) + b\tilde{k}_1 v_r + b\tilde{k}_2\Delta\left(d, t\right) + b\tilde{k}_3 \tag{2-38}$$

where $\tilde{k}_i = k_i - k_i^*$ (i=1,2,3). We rewrite $\Delta(d, t)$ as kd and denote $x_1 = v_r$ and $x_2 = d$. Now we have

$$\begin{cases} \dot{x}_1 = -a_m\left(x_1 + kx_2\right) - b\tilde{k}_1 x_1 - bk\tilde{k}_2 x_2 - b\tilde{k}_3 + u_1 \\ \dot{x}_2 = \left(1 - a_m H\right)x_1 - a_m kHx_2 - bH\tilde{k}_1 x_1 - bHk\tilde{k}_2 x_2 - bH\tilde{k}_3 - H_l u_1 \end{cases} \tag{2-39}$$

where $u_1 = \dot{v}_l$. Consider the following Lyapunov function

$$V = V_a + \sum_{i=1}^{3} \frac{b}{2g_i}\tilde{k}_i^2 \tag{2-40}$$

where V_a is the same as in (2-28). It is easy to verify by using the adaptive laws (2-37) and the knowledge of $k_i^* \in \left[k_{il}, k_{iu}\right]$ that

$$\dot{V} \le \dot{V}_a - \frac{b}{g_3}\tilde{k}_3\dot{k}_3^* \tag{2-41}$$

where $\dot{V}_a$ is given in (2-31) and

$$\dot{k}_3^* = \dot{u}_d - \frac{\dot{d}}{b} \tag{2-42}$$

Since $\dot{d}$, $\dot{v}_l$ are assumed to be bounded, it follows that $\dot{k}_3^*$ is bounded. It is easy to show that if all the conditions in (2-24a) - (2-24d) are satisfied then $\dot{V}$ is negative when x_1 or x_2 or both are large. This implies that V is bounded, and therefore all the signals in the closed-loop system are bounded.

When v_l and d are constants, $\dot{V} < 0$ when either x_1 or x_2 is nonzero. It is easy to verify that $x_1, x_2 \in L_2 \cap L_\infty$ and $\dot{x}_1, \dot{x}_2 \in L_\infty$. It follows from Barbalat's Lemma that $x_1, x_2 \to 0$ as $t \to \infty$, i.e., the control objective in (2-7) is achieved.

ÿ

In [23], an adaptive controller was proposed with the nonlinear time headway in (2-11), and the gain k was chosen as

$$k = c_k + (k_0 - c_k)e^{-sd^2} \tag{2-43}$$

where k_0, c_k, and s are positive constants to be designed (with $c_k < k_0$). Even though it was shown in [23] that such choice for h and k could lead to good platoon performance, the system stability was not established. However, k in (2-43) is bounded by c_k and k_0 all the time. Hence Lemma 2.3 points out that if we choose the parameters properly, the adaptive controller in (2-36) and (2-37) makes the closed-loop system stable with h and k as chosen in [23].

Since we have the flexibility to choose $\Delta(d, t)$, we can set $\Delta(d, t) = kd$ where k is a positive constant. Hence we have the following lemma, which is a special case of Lemma 2.3 with the fact that $k_l = k = k_u$. The proof follows the same steps as the proof for Lemma 2.3, and is omitted.

Lemma 2.4: Consider the system (2-2) - (2-4), with the control law

$$u = k_1 v_r + k_2 d + k_3 \tag{2-44}$$

where k_i the estimate of k_i^* (defined in Lemma 2.2) with initial condition k_{i0} (i =1,2,3) is generated according to the adaptive laws:

$$\begin{cases} \dot{k}_1 = \text{Proj}\{g_1 x_1[(p_1 x_1 + x_2) + (x_1 + a_m k p_1 x_2 + a_m x_2)H]\} \\ \dot{k}_2 = \text{Proj}\{g_2 x_2[(p_1 x_1 + x_2) + (x_1 + a_m k p_1 x_2 + a_m x_2)]\} \\ \dot{k}_3 = \text{Proj}\{g_3[(p_1 x_1 + x_2) + (x_1 + a_m k p_1 x_2 + a_m x_2)H]\} \end{cases} \tag{2-45}$$

where a_m, p_1, g_1, g_2 and g_3 are positive design parameters, and Proj{•} is defined in Lemma 2.3. All the signals in the closed-loop system are bounded if the design parameters are chosen such that

$$a_m p_1 > 1 \tag{2-46a}$$

$$\frac{4 p_1 k}{a_m + a_m k p_1 - k} > \sup H \tag{2-46b}$$

Furthermore, if v_l and d are constants, then the control objective in (2-7) is achieved, i.e. $v_r, d \to 0$ as $t \to \infty$.

ÿ

To avoid unnecessary switching between the brake and fuel systems, the following switching rules are incorporated in the vehicle following mode:

S1. If the separation distance x_r is larger than $x_{\max}$ ($x_{\max}>0$ is a design constant), then the fuel system is on.

S2. If the separation distance x_r is smaller than $x_{\min}$ ($x_{\min}>0$ is a design constant), then the brake system is on.

S3. If $x_{\max}\le x_r\le x_{\max}$, then the fuel system is on when $u>0$, while the brake system is on when $u<-u_0$ ($u_0>0$ is a design constant). When $-u_0\le u\le 0$, the brake system is inactive and the fuel system is operating as in idle speed.

These rules were successfully employed in PATH TO 4203 [31].

There are several other practical issues associated with the application of the controller (2-36) or (2-44). To guarantee that the constraints **C1**, **C2** are not violated, we should avoid the generation of high or fast varying control signals. Such high or fast varying control signals can be generated by the control law (2-36) or (2-44) if the lead vehicle accelerates rapidly or changes lanes creating a large spacing error or the ACC vehicle switches to a new target with large initial spacing error. The control parameter k shown in (2-43) is proposed in [23] to eliminate the adverse effects of large separation error. In [26], the nonlinear filter shown in Figure 3 is used to smooth the speed trajectory of the lead vehicle. The filtered speed trajectory $\hat{v}_l$ is then used by the controller. The $sat(d)$ function defined as

$$sat(d)=\begin{cases} e_{\max}, & \text{if } d > e_{\max} \\ e_{\min}, & \text{if } d > e_{\min} \\ d, & \text{otherwise} \end{cases} \tag{2-47}$$

is used instead of d in order to eliminate the adverse effects of large separation error. Furthermore, a low pass filter is placed before the throttle actuator so that fast varying commands will not be sent to the throttle system. The modifications in [26] are adopted in our vehicle following controllers and evaluated using simulations.

The following logic is used for the ACC system to switch between the speed tracking controller and vehicle following controller:

The speed tracking controller is active when no object is detected by the looking-forward sensor, or one object is detected with $v_l>v_d$ and $d>d_{n1}$ (v_d is set by the roadway controller, and d_{n1} is a negative design parameter), or one object is detected with $d>d_p$ (d_p is a positive design parameter). The vehicle following controller is active when $d<d_{n2}$ (d_{n2} is a negative design parameter and $d_{n2}<d<d_{n1}$). In all the other cases, the controller used in the previous time interval is employed.

This simple switching logic will be used in the integrated roadway/ACC system so that all ACC vehicles can interact with the roadway controller in a safe manner.

2.4.3 Simulations

In this section, we present the simulation results that demonstrate the performance of the vehicle following controller given by (2-44) when applied to the validated nonlinear vehicle model used in [26]. The variable time headway given in (2-13) is used for control design and the control parameters are chosen as

$s_0 = 5\text{m}$, $h_1 = 0.5$, $h_2 = 0.016$, $v_{\max} = 30$, $k = 0.2$, $a_m = 2$, $p_1 = 20$
$e_{\max} = 10\text{m}$, $e_{\min} = -30\text{m}$, $a_{\max} = 1.0\text{m/s}^2$, $a_{\min} = -2.0\text{m/s}^2$, $p = 10$
$k_{10} = 10$, $k_{1u} = 16$, $k_{1l} = 4$,
$k_{20} = 2$, $k_{2u} = 2.8$, $k_{2l} = 0.6$,
$k_{30} = 0$, $k_{3u} = 30$, $k_{3l} = -30$,
$g_1 = 1.4$, $g_2 = 0.2$, $g_3 = 0.6$

It can be seen that the safety spacing in (2-17) is not violated and the parameters satisfy the conditions given by (2-25), (2-46a) and (2-46b). In simulations 3 and 4, the Pipes' vehicle following model [35] is chosen among several other vehicle following models to simulate manually driven passenger vehicles, as it simulates slinky type effects that are often observed in actual vehicle following [9, 33]. It is a linear follow-the-leader model based on vehicle following theory that pertains to a single lane dense traffic with no passing and assumes that each driver reacts to the stimulus from the vehicle ahead. The transfer function of the Pipes' model is given by

$$G_p(s) = \frac{v_i}{v_{i-1}} = \frac{Ke^{-ts}}{s + Ke^{-ts}} \tag{2-48}$$

with v_{i-1} and v_i are the speeds of the lead and following vehicles, respectively, $t = 1.5\text{sec}$ and $K = 0.37\text{sec}^{-1}$ [9, 33].

Simulation 1

Two vehicles are used to evaluate the vehicle following properties of the proposed controller. The following vehicle is equipped with the ACC controller (vehicle following controller in (2-44)). The speed, acceleration, speed error, separation error, throttle angle and brake pressure responses are presented in Figures 4(a)-(f), respectively.

At time zero, the two vehicles have zero speed and are separated with a distance of s_0. From t = 0s to t = 20s, the lead vehicle increases its speed with a constant acceleration 0.8m/s^2, and then cruises at 16m/s. From t = 50s to t = 53s, the lead vehicle increases its speed with a constant acceleration 2.0m/s^2, and then cruises at 22m/s. From t = 90s to t = 100s, the lead vehicle increases its speed with a constant acceleration 0.6m/s^2, and then cruises at 28m/s. From t = 140s to t = 144s, the lead vehicle decreases its speed deceleration –2.0m/s^2, and then cruises at 20m/s. As we can see, when the acceleration of the lead vehicle is not too large (0.8 or 0.6m/s^2), the throttle controller regulates the fuel

system smoothly and the ACC vehicle follows the lead vehicle with small speed and separation errors. These errors are regulated towards zero when the lead vehicle reaches a constant speed. When the acceleration of the lead vehicle is large ($2.0 m/s^2$) for a short time, the following vehicle increases its speed in a smooth and comfortable way. The transient speed and separation errors are large due to the high acceleration of the lead vehicle. However, the errors are regulated towards zero as soon as the lead vehicle reaches a constant speed. When the lead vehicle decreases its speed rapidly, the brake system on the ACC vehicle is active and the brake pressure is shown in Figure 4(f). From the acceleration and separation error responses, we can see that the ACC system works in a comfortable and safe way.

(a)

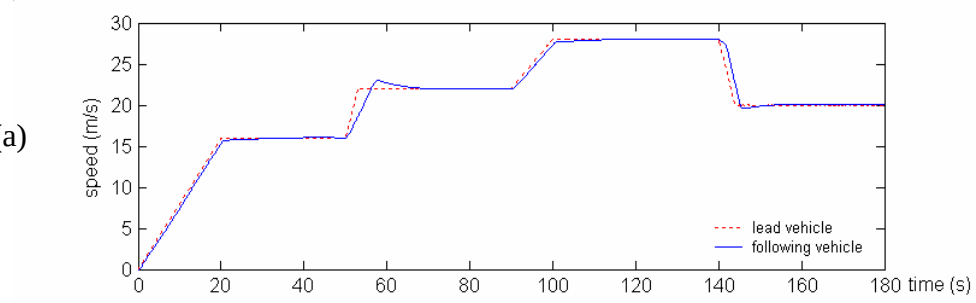
speed (m/s)
time (s)
lead vehicle
following vehicle

(b)

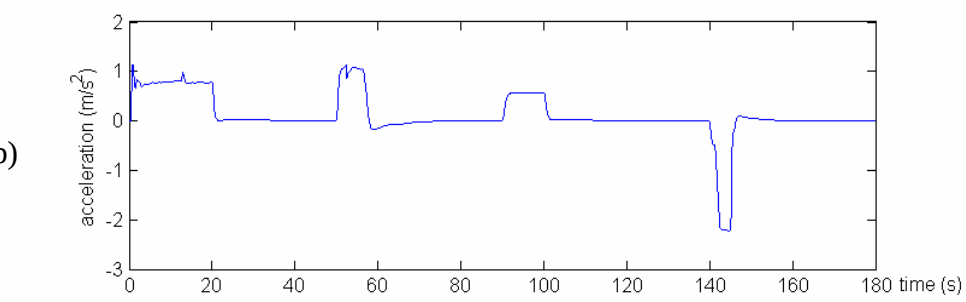
acceleration (m/s2)
time (s)

(c)

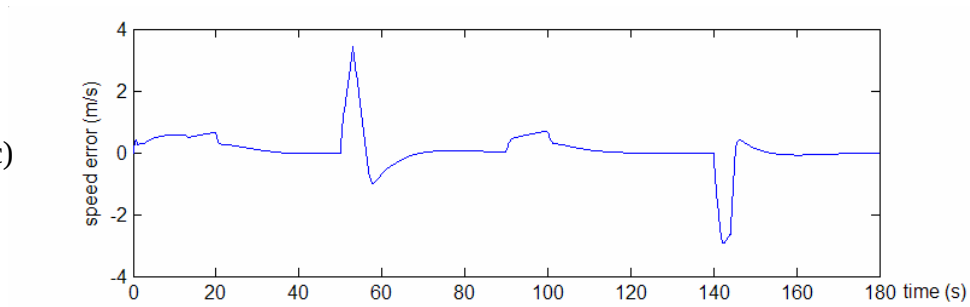
speed error (m/s)
time (s)

(d)

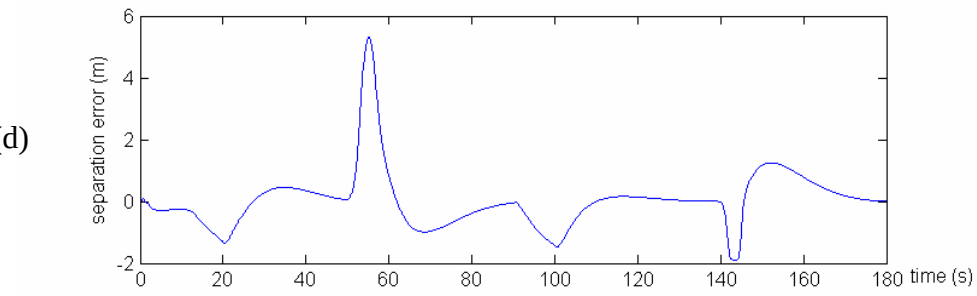
separation error (m)
time (s)

(e)

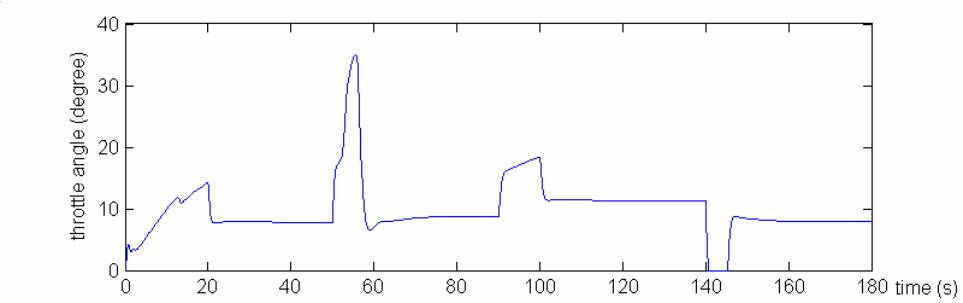

(f)

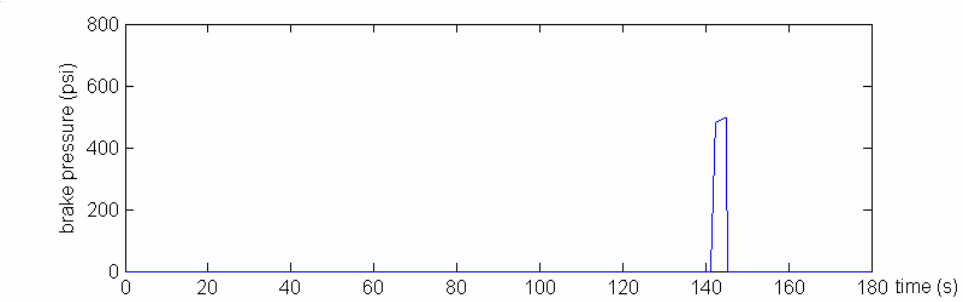

Figure 4. Responses of the following ACC vehicle: (a) speed, (b) acceleration, (c) speed error, (d) separation error, (e) throttle angle and (f) brake pressure in Simulation 1.

Simulation 2

This simulation is used to demonstrate that the proposed vehicle following controller in (2-44) guarantees string stability. In this simulation five vehicles are simulated in a vehicle following scenario. The lead vehicle generates the speed trajectory shown as a red dotted line in Figure 5(a). The four following vehicles are ACC vehicles. The speed, speed error, and separation error responses of the ACC vehicles are shown in Figures 5(a)-(c), respectively. As we can see the speed and separation errors are attenuated within the vehicle string when the brake system is not activated. When the lead vehicle begins to decelerate rapidly, the speed and separation errors are not attenuated within the vehicle string. This is because the switching logic introduces a hysteresis effect in the ACC system. However, the errors are still propagated in a satisfactory manner.

(a)

(b)

(c)

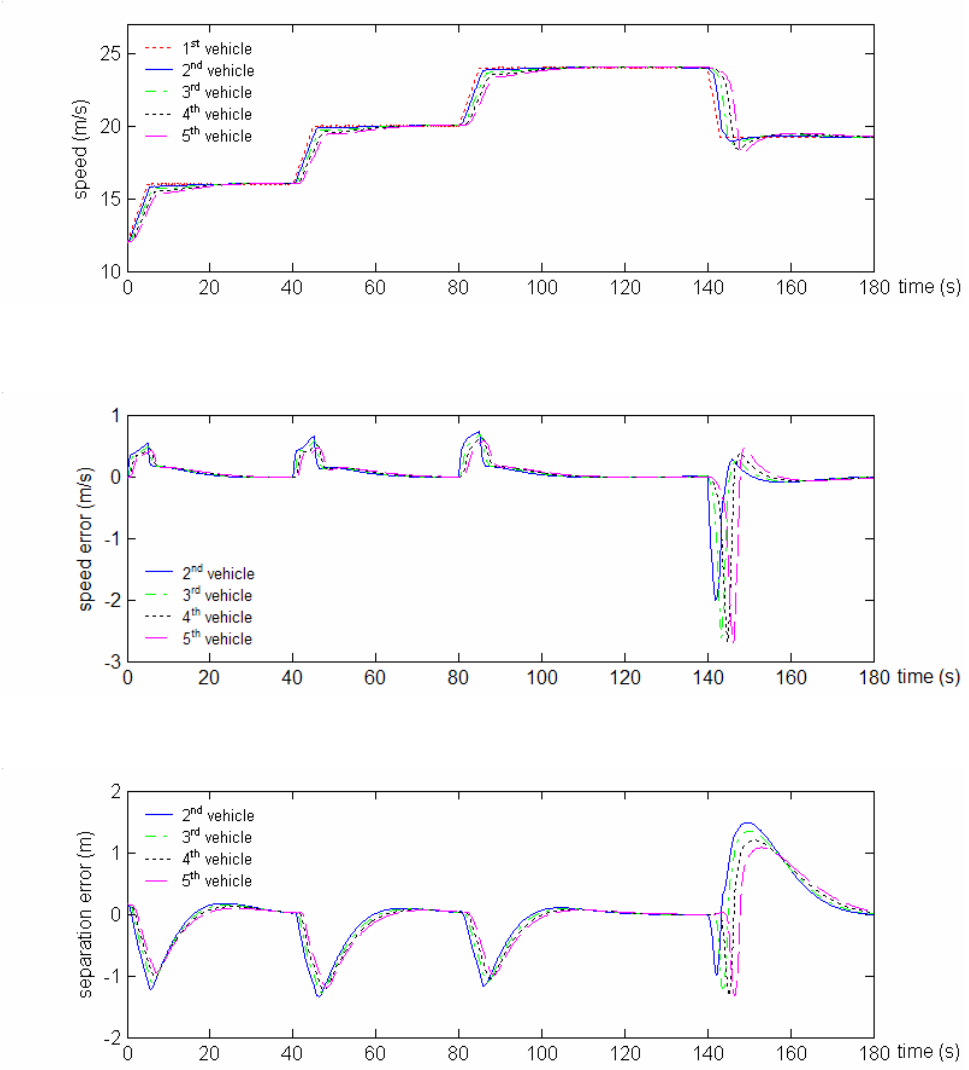

Figure 5. Responses of the following ACC vehicles: (a) speed, (b) speed error and (c) separation error in Simulation 2.

Simulation 3

Despite previous modifications in the vehicle following controller to take care of the acceleration and jerk constraints, under certain conditions, the constraints **C1** and **C2** may still get violated. This simulation demonstrates this flaw.

In this simulation, ten vehicles are simulated and the ACC vehicle is in the second position. The other eight vehicles following the ACC vehicle are manually driven passenger vehicles simulated using the Pipes' model (2-48). At time zero, all the vehicles have zero speed. From t = 0s to t = 6s, the lead vehicle increases its speed with a constant acceleration 2m/s^2, and then cruises at 12m/s. From t = 50s to t = 56s, the lead vehicle increases its speed with a constant acceleration 2.0m/s^2, and then cruises at 24m/s. The speeds, acceleration, speed error, separation error responses are presented in Figures 6(a)-(d), respectively. Though the control objective is achieved, the ACC vehicle accelerates in an aggressive manner, as shown in Figure 6(b). This is because when the preceding vehicle accelerates rapidly, large speed error may appear temporarily and cause fast varying separation error. Hence the separation error should also be filtered in a proper way so that fast varying control effort is avoided and the control objective is achieved.

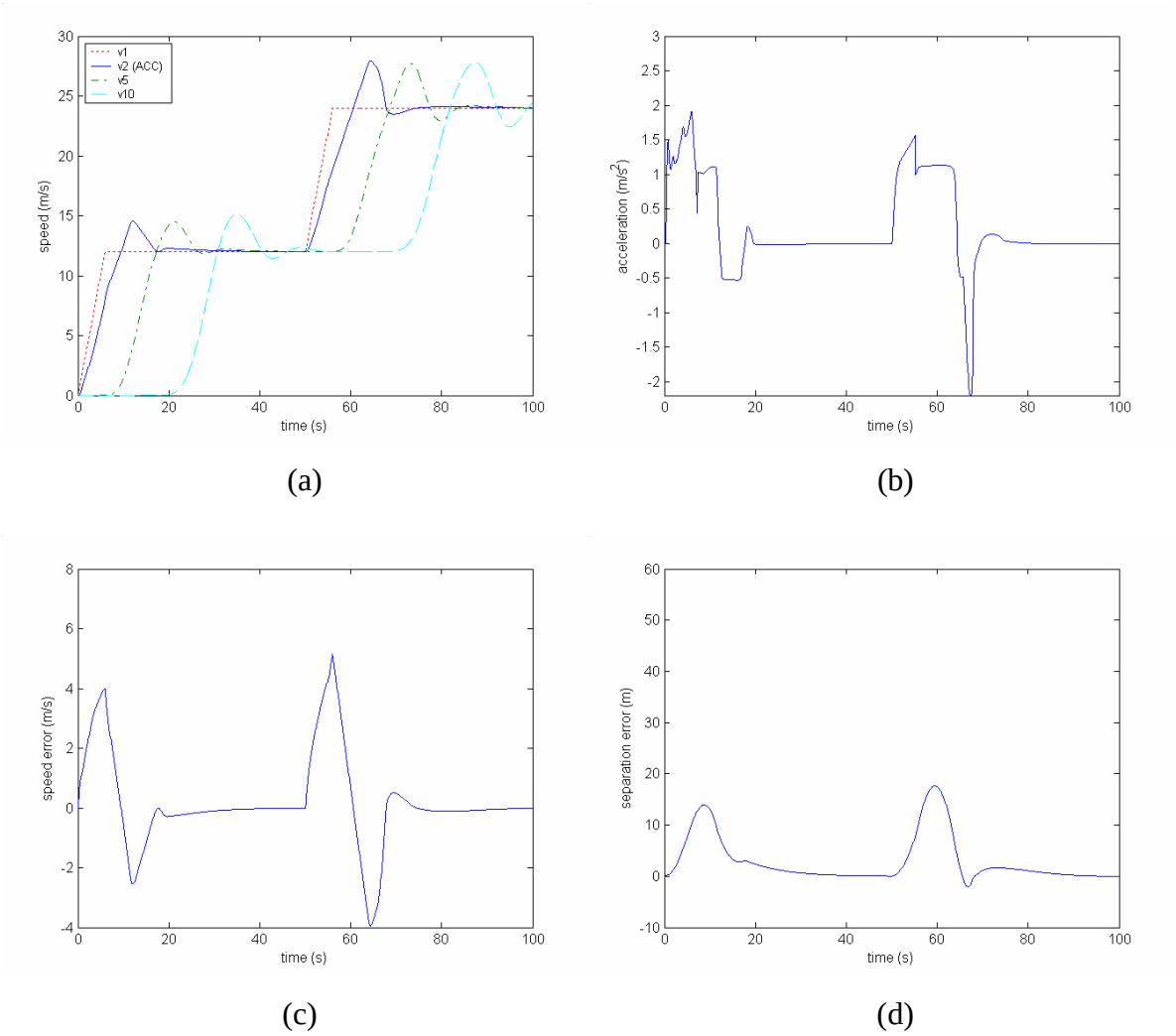

Figure 6. (a) Speed responses in the vehicle string, and responses of the ACC vehicle: (b) acceleration, (c) speed error and (d) separation error in Simulation 3.

Simulation 4

This simulation is similar to Simulation 3. However, in this simulation the lead vehicle accelerates in an aggressive manner and its speed oscillates before settling to a constant value. This situation may arise in today's traffic where traffic disturbances downstream create a situation where the driver speeds up and then slows down in an oscillatory fashion before reaching steady state. In this situation, the temporary separation distance between the first and second vehicles will be large, and we would like to investigate how the vehicle equipped with controller (2-44) will behave with respect to the high acceleration and speed oscillations of the lead vehicle.

At time t = 0s the lead vehicle begins to accelerate from 0m/s with a constant acceleration of 2.0m/s^2 for 6 seconds, and its speed oscillates around 12m/s before settling to the constant speed of 12m/s. At time t = 50second, the lead passenger vehicle accelerates again with 2.0m/s^2 for another 6 seconds and its speed oscillates around 24m/s before settling to the constant. The speeds, acceleration, speed error, separation error responses are presented in Figures 7(a)-(d), respectively. As we can see, the ACC vehicle accelerates aggressively and the oscillations in the speed of the lead vehicle are unattenuated along the vehicle string.

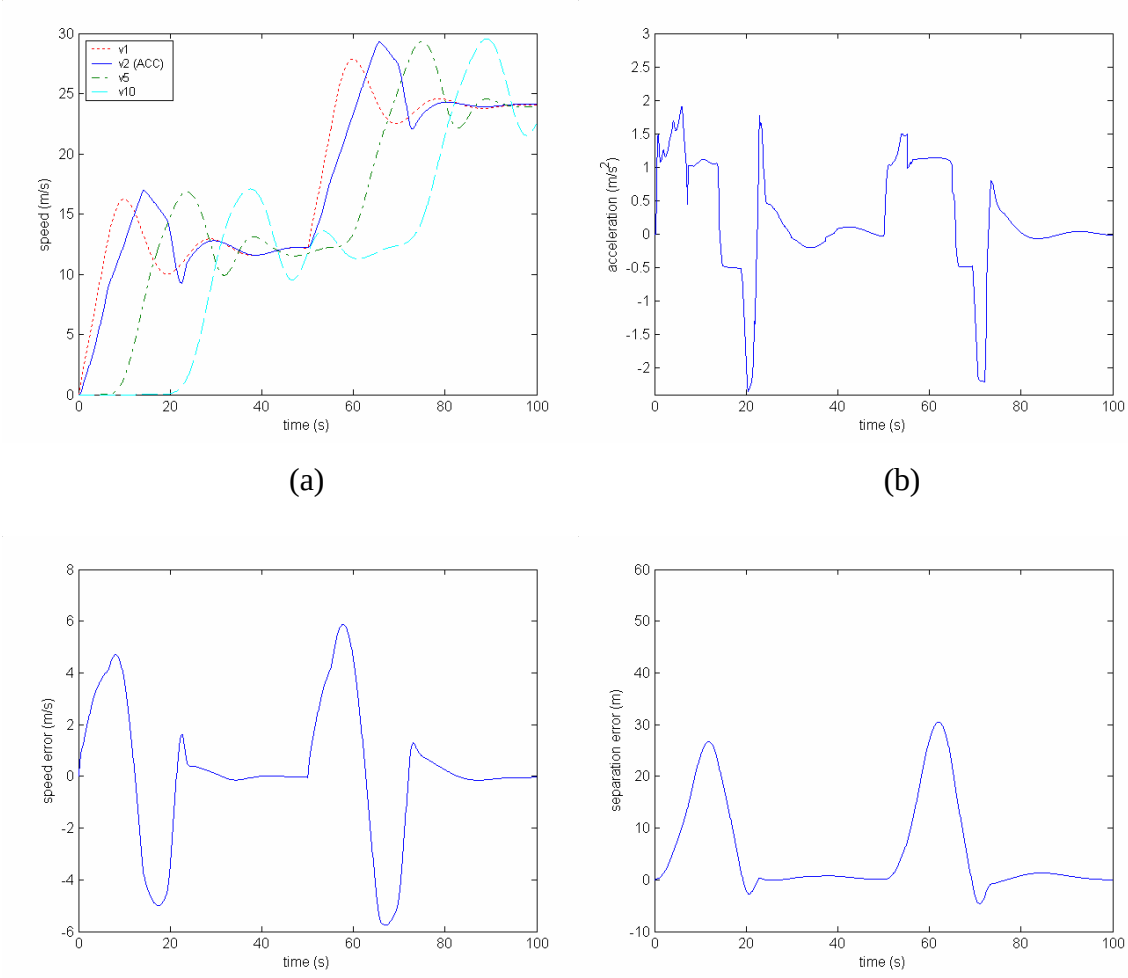

Figure 7. (a) Speed responses in the vehicle string, and responses of the ACC vehicle: (b) acceleration, (c) speed error and (d) separation error in Simulation 4.

The above simulations demonstrate that the adaptive vehicle following controller (2-44) can guarantee system stability and provide good transient response under normal driving conditions. However, when the preceding vehicle accelerates rapidly, the fast increasing v_l may also lead to fast increasing d since the ACC vehicle is not allowed to accelerate rapidly. This fast increasing d may cause high control effort (as shown in Simulation 3 in the previous section). When the separation error is very large, it may take long time for the ACC vehicle to catch the preceding vehicle. If we simply use $sat(d)$ for the controller (2-44), any changes in v_l will affect the control signal when $d>sat(d)$, while some changes in v_l may be ignored. In the next section we design the ACC controller to address these issues in addition to others.

2.5 ACC Design Strategy 2: Disturbance Rejection

In the previous section, we have shown that the controllers in (2-36) or (2-44) can guarantee system stability and provide satisfactory transient performance under normal driving conditions (see Simulations 1 and 2). However, under some extreme conditions, they cannot guarantee good transient performance and the oscillations in v_l affect the following vehicle's speed without any attenuation, even though the separation error is very large. This class of ACC systems has very similar properties to the ACC systems proposed in the literature.

In this section, we design an ACC system that can use the knowledge of v_l and d and provide better transient responses than those in (2-36) or (2-44) in the presence of traffic disturbances. In the report for PATH TO 4203 [31], a vehicle following controller is proposed for heavy trucks to reject high frequency disturbances in the speed of the lead vehicle. This controller converts the vehicle following task to a special speed tracking task, and has been shown to guarantee good transient responses and better fuel economy. In this subsection, we design the ACC system based on the same motivation but with different control design methodology. The ACC system designed in this subsection can guarantee global stability, in contrast to only local stability established for the ACC system in [31].

2.5.1 ACC Design

The following lemma establishes that the vehicle following task is a special speed tracking task.

Lemma 2.5: For the vehicle following task described in section 2.2, if the controller is designed such that $v_r + kd \to 0$ as $t \to \infty$ (k is a positive constant) and $\frac{d}{dt}(v_r + kd)$ is uniformly continuous, then v_r and d are bounded. In addition, if v_l is a constant, then the control objective in (2-7) is achieved.

Proof: If $\frac{d}{dt}(v_r + kd)$ is uniformly continuous and $v_r + kd \to 0$ then it follows from Barbalat's Lemma, that $\frac{d}{dt}(v_r + kd) \to 0$ as $t \to \infty$ and therefore

$$\frac{d}{dt}\left(v_r + kd\right) = \left(1 + kH\right)\dot{v}_r + kv_r - k\left(H + H_l\right)\dot{v}_l \to 0 \tag{2-49}$$

as $t \to \infty$. It also follows from $\frac{d}{dt}(v_r + kd)$ being uniformly continuous and $\frac{d}{dt}(v_r + kd) \to 0$ as $t \to \infty$ that $\frac{d}{dt}(v_r + kd)$ is bounded. Since k is a positive constant, $H > 0$, and H, H_l and $\dot{v}_l$ are bounded, it follows that v_r is bounded. In addition $v_r + kd$ is uniformly continuous since $\frac{d}{dt}(v_r + kd)$ is bounded. Hence it can be shown that $(v_r + kd)$ is bounded since it is uniformly continuous and converges to zero. Hence d is bounded. In particular, if v_l is a constant, then (2-49) implies $v_r \to 0$ and therefore $d \to 0$ which in turn implies that the control objective in (2-7) is achieved.

ÿ

Lemma 2.5 indicates that the vehicle following task can be viewed as a special speed tracking task, in which the desired speed v_d is equal to $v_l + kd$. If we can design the vehicle following controller such that $v \to v_l + kd$ in a proper way (for example, keeping $\frac{d}{dt}(v_r + kd) \to 0$ at the same time), then v_r and d are guaranteed to be bounded, and the control objective in (2-7) can be achieved when v_l is a constant. We propose the speed tracking controller

$$u = f_u^{-1}\left(v_{ref}\right) + k_1 e_v + k_2 + k_3 \dot{v}_{ref} \tag{2-50}$$

where $e_v = v_{ref} - v$, v_{ref} is the reference speed, and the control parameters k_i (i =1,2,3) are updated by

$$\begin{cases} \dot{k}_1 = \mathrm{Proj}\{g_1 e_v^2\} \\ \dot{k}_2 = \mathrm{Proj}\{g_2 e_v\} \\ \dot{k}_3 = \mathrm{Proj}\{g_3 e_v \dot{v}_{ref}\} \end{cases} \tag{2-51}$$

In (2-51) g_i (i =1,2,3) are positive design parameters, and the function Proj{·} limits k_i between their lower bounds k_{il} and upper bounds k_{iu} (i =1,2,3). Note, the control gains k_i (i =1,2,3) are different from those used in controller (2-36) or (2-44).

Lemma 2.6: Consider the system in (2-2) - (2-4) with the controller in (2-50) and the update laws in (2-51). If k_{li} and k_{ui} (i =1,2,3) are properly chosen, then all the signals in the closed-loop system are bounded. In addition:
(i) If d is a constant, $e_v \to 0$ as $t \to \infty$.
(ii) If d is a constant and $\dot{v}_{ref}$ is uniformly continuous, $e_v, \dot{e}_v \to 0$ as $t \to \infty$.

Proof: For the system represented in (2-2) - (2-4), if *a*, *b* and *d* are known, then the controller can be designed as

$$u = f_u^{-1}\left(v_{ref}\right) + k_1^* e_v + k_2^* + k_3^* \dot{v}_{ref} \tag{2-52}$$

where $k_1^* = \frac{a_m - a}{b}$, $k_2^* = -\frac{d}{b}$, $k_3^* = \frac{1}{b}$ and a_m is a positive constant. In this case the close-loop system becomes

$$\dot{e}_v = -a_m e_v \tag{2-53}$$

Hence, $e_v, \dot{e}_v \to 0$ as $t \to \infty$. Since *a*, *b* and *d* are unknown, the control law (2-50) is proposed, and the closed-loop system can be rewritten as

$$\dot{e}_v = -a_m e_v - b\tilde{k}_1 e_v - b\tilde{k}_2 - b\tilde{k}_3 \dot{v}_{ref} \tag{2-54}$$

Consider the following candidate Lyapunov function

$$V = \frac{e_v^2}{2} + \frac{b\tilde{k}_1^2}{2g_1} + \frac{b\tilde{k}_2^2}{2g_2} + \frac{b\tilde{k}_3^2}{2g_3} \tag{2-55}$$

If k_{li} and k_{ui} are chosen such that $k_{li} \le k_i^* \le k_{ui}$ is true for each *i*, then with the update law in (2-51), it can be shown that

$$\dot{V} = e_v \dot{e}_v + \frac{b}{g_1}\tilde{k}_1\dot{\tilde{k}}_1 + \frac{b}{g_2}\tilde{k}_2\dot{\tilde{k}}_2 + \frac{b}{g_3}\tilde{k}_3\dot{\tilde{k}}_3 \le -a_m e_v^2 + \frac{1}{g_2}\tilde{k}_2\dot{d} \tag{2-56}$$

It can be shown [34] that e_v and all signals are bounded. (2-56) also implies that if *d* is a constant, then $e_v \in L_2 \cap L_\infty$ and $\dot{e}_v \in L_\infty$, which implies $e_v \to 0$. Furthermore, if $\dot{v}_{ref}$ is uniformly continuous, it can be verified that $\dot{e}_v$ is also uniformly continuous. Using Barbalat's Lemma, we can show that $\dot{e}_v$ also converges to zero.

ÿ

Since the selected desired speed $v_l + kd$ may vary fast, we employ the nonlinear filter in Figure 8 to generate a smooth signal v_{ref} to be tracked. The saturation function inside the nonlinear filter serves as an acceleration limiter that restricts the rate of change of v_{ref} between $a_{\min}$ and $a_{\max}$. The signal generated by the acceleration limiter is $z = sat\{p(v_l + kd - v_{ref})\}$, where *p* is a positive design parameter. The function after the acceleration limiter is designed to accept or ignore the change rate signal *z*, and is given as

$$f\left(z, v_{ref}, v_l\right) = \begin{cases} z, & \text{if } v_l + m_v \le v_{ref} \le v_l + M_v \text{ and } z < 0; \\ & \text{or } v_l - m_v < v_{ref} < v_l + m_v; \\ & \text{or } v_{ref} \le v_l - m_v \text{ and } z > 0 \\ 0, & \text{if } v_l + m_v \le v_{ref} \le v_l + M_v \text{ and } z \ge 0; \\ & \text{or } v_{ref} \le v_l - m_v \text{ and } z \le 0 \\ a_{\min}, & \text{if } v_{ref} > v_l + M_v \end{cases} \tag{2-57}$$

where m_v and M_v are constant design parameters with $0 < m_v < M_v$. When $v_l - m_v < v_{ref} < v_l + m_v$, which means the reference speed for the following vehicle is not too low or too high, v_{ref} can vary with any value provided by z. If v_l increases and stays at some constant value, v_{ref} will never exceed $v_l + m_v$. Similarly if v_l decreases and stays at some constant value, v_{ref} will never be lower than $v_l - m_v$. If for some reasons the condition $v_l + m_v \le v_{ref} \le v_l + M_v$ is satisfied (for example, the preceding vehicle slows down), then v_{ref} decreases when $v_{ref} > v_l + kd$, or remains constant when $v_{ref} \le v_l + kd$. If $v_{ref} \le v_l - m_v$ is true, then v_{ref} increases when $v_{ref} > v_l + kd$, or remains constant otherwise. In the last case, when $v_{ref} > v_l + M_v$, v_{ref} decreases with the deceleration $a_{\min}$ to avoid a higher than the limit reference speed.

As we can see, this nonlinear filter limits the rate of change of v_{ref} between $a_{\min}$ and $a_{\max}$, and prevents regulating v_{ref} much higher or lower than v_l. In some situations, this nonlinear filter ignores some unnecessary changes in v_{ref} and generates constant reference speeds. By regulating the ACC vehicle's speed towards v_{ref}, the ACC system forces the vehicle to follow the preceding vehicle in a safe and comfortable way, and the control objective in (2-9) is still achievable. The acceleration limits $a_{\min}$ and $a_{\max}$ are chosen based on the constraint **C1** and the vehicle dynamics.

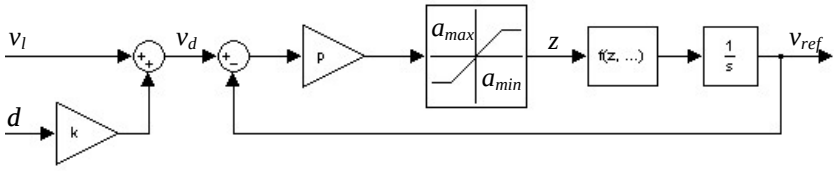

Figure 8. Nonlinear filter used in the new ACC design for disturbance rejection.

Remark 2.1: Even though the signal z within the nonlinear filter in Figure 8 is continuous, the function (2-57) may generate discontinuous signals, which may cause problems in the analysis related to the existence and uniqueness of solutions to the resulting differential equation. The discontinuities may arise when v_{ref} varies around $v_l - m_v$, or $v_l + m_v$ or $v_l + M_v$. However, the function (2-57) can be slightly modified so that it will always generate continuous signals when z is continuous. For example, we can choose a small positive constant e, and when z>0 and $v_l + m_v - e \le v_{ref} < v_l + m_v$ are

satisfied, we set f equal to $(v_l + m_v - v_{ref})\cdot z/e$ instead of z. In such a way, discontinuous signals will not be generated when v_{ref} varies around $v_l + m_v$.

Lemma 2-7: Consider the system in (2-2) - (2-4) with the controller in (2-50) and the update laws in (2-51). If k_{li} and k_{ui} (i =1,2,3) are properly chosen and v_{ref} is generated by the nonlinear filter in Figure 8, then u, v and v_r are bounded. In addition:
(i) If d is a constant, $v \to v_{ref}$ and $\dot{v} \to \dot{v}_{ref}$ as $t \to \infty$.
(ii) If v_l and d are constants, and the control parameters are chosen such that

$$(1/k + \inf H)|a_{\min}| > m_v \tag{2-58a}$$

$$(1/k + \inf H)a_{\max} > m_v \tag{2-58b}$$

where inf H is the infimum of H, then all the signals in the closed-loop system are bounded.

Proof: With the function in (2-57), it is easy to see that $|v_l - v_{ref}|$ is bounded from above by $\max\{|v_l(0)-v_{ref}(0)|, M_v\}$. Since we can always set $v_{ref}(0) = v_l(0)$, it can be concluded that $|v_l - v_{ref}|$ is bounded by M_v. It is followed from Lemma 2-7 that $(v - v_{ref})$ is bounded, which implies that v_r is bounded. Using the fact that v_l is bounded, it is easy to show that u, v are bounded. It can be shown that $\frac{d}{dt}(v_l + kd)$ is bounded, so it follows that $v_l + kd$ is uniformly continuous. It is verified that $\dot{v}_{ref}$ generated by (2-57) (with modifications suggested in Remark 2.1) is also uniformly continuous. Hence part (i) can be proven using Lemma 2-6. For part (ii), when v_l and d are constants, we consider the following Lyapunov function:

$$V = \tfrac{1}{2}x^T Px + \frac{b\tilde{k}_1^2}{2g_1} + \frac{b\tilde{k}_2^2}{2g_2} + \frac{b\tilde{k}_3^2}{2g_3} \tag{2-59}$$

where $P = \begin{bmatrix} 1/k + 1/p & 1 \\ 1 & k \end{bmatrix} > 0$, and $x = [v_l - v_{ref}, d]^T$. Hence,

$$\begin{aligned} \dot{V} = &-[(1/k + 1/p + H)x_1 + (1 + kH)x_2]\dot{x}_1 \\ &+ (x_1 + kx_2)x_1 + (x_1 + kx_2)(h_1 + Hh_2) \end{aligned} \tag{2-60}$$

In the following analysis, we only consider the situations in which $v_l - m_v \le v_{ref} \le v_l + m_v$ is satisfied since v_{ref} will be bounded by $v_l - m_v$ and $v_l + m_v$ in finite time for any bounded initial conditions.

? For $v_l - m_v < v_{ref} < v_l + m_v$, or $v_{ref} = v_l + m_v$ and $z \le 0$, or $v_{ref} = v_l - m_v$ and $z \ge 0$:
In this case, $\dot{x}_1 = -z = -sat\{p(x_1 + kx_2)\}$. Hence

$$\begin{aligned}\dot{V} &= -\left[(1/k + 1/p + H)x_1 + (1 + kH)x_2\right]\text{sat}\{p(x_1 + kx_2)\} \\ &+ (x_1 + kx_2)x_1 + (x_1 + kx_2)(h_1 + Hh_2) \\ &= -(1/k + H)(x_1 + kx_2)\text{sat}\{p(x_1 + kx_2)\} \\ &- (1/p)x_1\text{sat}\{p(x_1 + kx_2)\} + (x_1 + kx_2)x_1 \\ &+ (x_1 + kx_2)(h_1 + Hh_2)\end{aligned} \tag{2-61}$$

If $a_{\min} \le p(x_1 + kx_2) \le a_{\max}$, then (2-61) becomes

$$\dot{V} = -p(1/k + H)(x_1 + kx_2)^2 + (x_1 + kx_2)(h_1 + Hh_2) \tag{2-62}$$

In this case $\dot{V} < 0$ if $|x_1 + kx_2| > |h_1 + h_2H|/[p(1/k+H)]$. If $p(x_1+kx_2) > a_{\max}$, then (2-61) becomes

$$\begin{aligned}\dot{V} &= -(1/k + H)(x_1 + kx_2)a_{\max} - (1/p)x_1 a_{\max} \\ &+ (x_1 + kx_2)x_1 + (x_1 + kx_2)(h_1 + Hh_2)\end{aligned} \tag{2-63}$$

It is easy to verify that when t is sufficiently large and (2-58b) is satisfied, $\dot{V} < 0$ always holds in this case. If $p(x_1+kx_2) < a_{\min}$, it can also be verified that when t is sufficiently large and (2-58a) is satisfied, $\dot{V} < 0$ always holds.

? For $v_{ref} = v_l + m_v$ and $z>0$:
In this case, $x_1 = -m_v$, $x_1 + kx_2 \ge z > 0$ and $\dot{x}_1 = -z = 0$. Hence

$$\dot{V} = -(x_1 + kx_2)m_v + (x_1 + kx_2)(h_1 + Hh_2) \tag{2-64}$$

When t is sufficiently large, $m_v > |h_1 + h_2H|$ always holds, which indicates that $\dot{V} < 0$ in this case.

? For $v_{ref} = v_l + m_v$ and $z>0$:
Following the same arguments as above it can be shown that $\dot{V} < 0$ holds for this case when t is sufficiently large.

We have shown that as $t \to \infty$, $\dot{V}$ might be positive only when $|x_1 + kx_2| < |h_1 + h_2H|/[p(1/k+H)]$. Since we have shown that x_1 is bounded, it is easy to conclude that V is bounded and all the signals inside the closed-loop system are bounded.

ÿ

Remark 2.2: In the proof for Lemma 2-7, we have assumed that (2-57) always generates continuous signals when z is continuous. One can verify that using the modifications for (2-57) suggested in Remark 2.1, the proof for Lemma 2-7 can be achieved in a similar way but with more regions for v_{ref}.

Remark 2.3: If h_1 and h_2 are zero in (2-60), it can be shown that x_1, $x_2 \to 0$ as $t \to \infty$, i.e. the control objective in (2-7) is achieved. The simulation results demonstrate that (2-7) can be achieved when v_l is a constant, even though we cannot prove it analytically in Lemma 2-7.

The new ACC system consists of two reference speed generators and the speed tracking controller (2-50) with the update laws (2-51). The nonlinear filter in Figure 3 is used as the reference generator in the speed tracking mode, while the nonlinear filter in Figure 8 is used in the vehicle following mode. The following switching rules are incorporated in the ACC system:

(In the vehicle following mode)
S1. If the separation distance x_r is larger than $x_{\max}$ ($x_{\max}>0$ is a design constant), then the fuel system is on.
S2. If the separation distance x_r is smaller than $x_{\min}$ ($x_{\min}>0$ is a design constant), then the brake system is on.
S3. If $x_{\max} \le x_r \le x_{\max}$, then the fuel system is on when $u>0$, while the brake system is on when $u<-u_0$ ($u_0>0$ is a design constant). When $-u_0 \le u \le 0$, the brake system is inactive and the fuel system is operating as in idle speed.

(In the speed tracking mode)
S4. The fuel system is on when $u>0$, while the brake system is on when $u<-u_0$. When $-u_0 \le u \le 0$, the brake is off and the fuel system is operating as in idle speed.

The ACC system designed in this subsection can be easily integrated with a roadway controller to receive desired speed commands send out to all ACC vehicles by the roadway. In real time implementation, the two reference speed generators work in parallel. The lower reference speed and its derivative are passed to the speed tracking controller. In this way, the ACC vehicle will follow the preceding vehicle in a safe manner and without violating the speed limit set by the roadway controller.

2.5.2 Comparison Simulations

In this section, we perform simulations to demonstrate the performance of the ACC system given in (2-50) with the update laws in (2-51). For comparison purpose, the four simulations conducted in section 2.4.3 are repeated here with the ACC system developed in section 2.5.1. For easy reference, we use ACC01 to represent the ACC system designed and tested in section 2.4 and ACC02 for the one designed in section 2.5.1. The variable time headway given in (2-13) is used for control design and the control parameters are chosen as

$s_0 = 5\text{m}$, $h_1 = 0.5$, $h_2 = 0.016$, $v_{\max} = 30$, $k = 0.2$,
$m_v = 2\text{m/s}$, $M_v = 8\text{m/s}$, $a_{\max} = 1.0\text{m/s}^2$, $a_{\min} = -2.0\text{m/s}^2$, $p = 10$
$k_{10} = 6$, $k_{1u} = 16$, $k_{1l} = 6$,
$k_{20} = 0$, $k_{2u} = 30$, $k_{2l} = -30$,

$k_{30} = 4$, $k_{3u} = 8$, $k_{3l} = 2$,
$g_1 = 5$, $g_2 = 0.8$, $g_3 = 0.4$

It can be seen that the control parameters are chosen such that the conditions given by (2-58a) and (2-58b) are satisfied.

Simulation C1

Two vehicles are used to evaluate the vehicle following properties of the proposed ACC system. The following vehicle is equipped with ACC02.

At time zero, the two vehicles have zero speed and are separated with a distance of s_0. From t = 0s to t = 20s, the lead vehicle increases its speed with a constant acceleration 0.8m/s^2, and then cruises at 16m/s. From t = 50s to t = 53s, the lead vehicle increases its speed with a constant acceleration 2.0m/s^2, and then cruises at 22m/s. From t = 90s to t = 100s, the lead vehicle increases its speed with a constant acceleration 0.6m/s^2, and then cruises at 28m/s. From t = 140s to t = 144s, the lead vehicle decreases its speed deceleration –2.0m/s^2, and then cruises at 20m/s. The speed, acceleration, speed error, separation error, throttle angle and brake pressure responses are presented in Figures 9(a)-(f), respectively. As we can see, ACC02 works in a comfortable and safe way, and its transient performance is almost the same as that of ACC01 in this case.

(a)

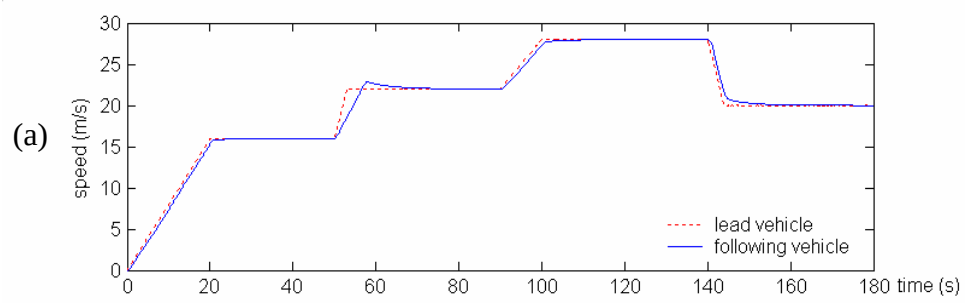
speed (m/s)
time (s)
lead vehicle
following vehicle

(b)

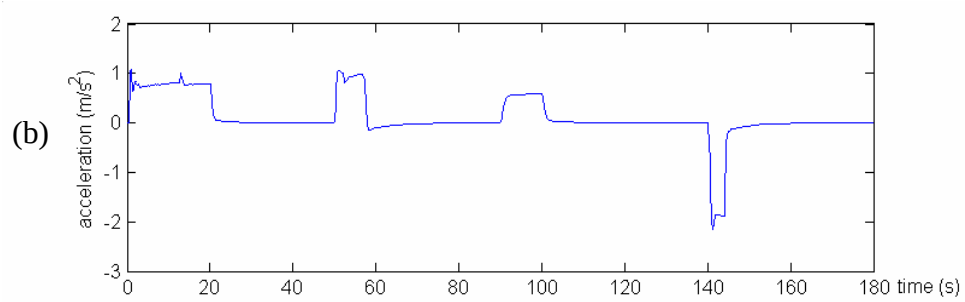
acceleration (m/s2)
time (s)

(c)

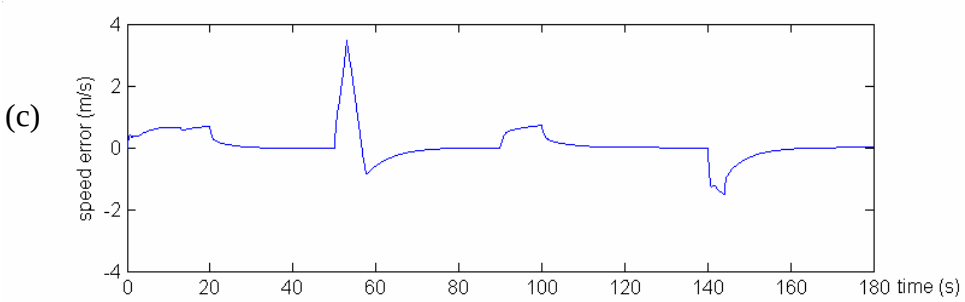
speed error (m/s)
time (s)

(d)

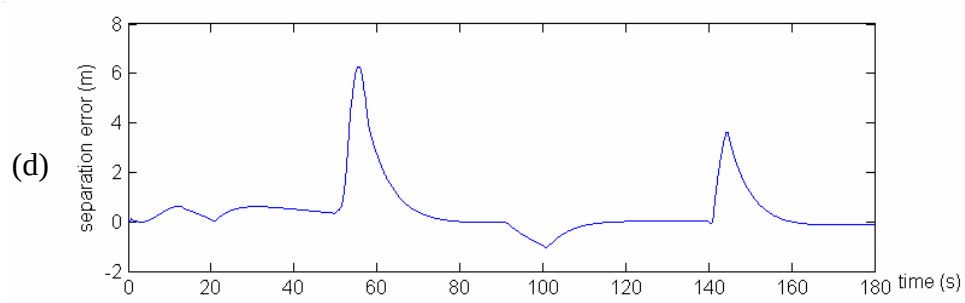
separation error (m)
time (s)

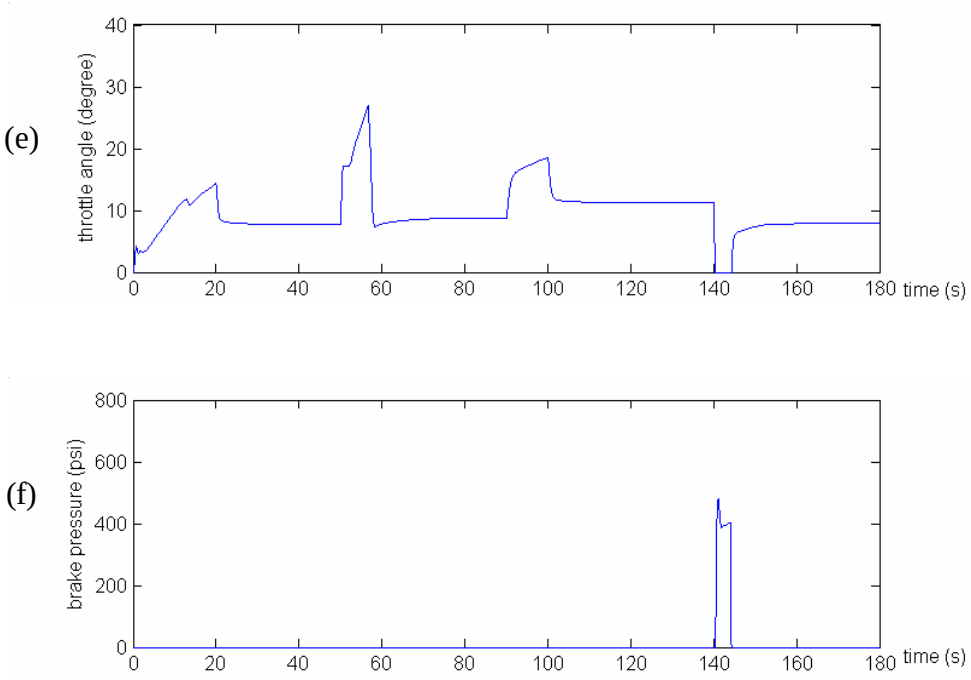

Figure 9. Responses of the following ACC vehicle: (a) speed, (b) acceleration, (c) speed error, (d) separation error, (e) throttle angle and (f) brake pressure in Simulation C1.

Simulation C2

In this simulation five vehicles are simulated in a vehicle following scenario. The lead vehicle generates the speed trajectory shown as a red dotted line in Figure 10(a), and the four following vehicles are equipped with ACC02. The speed, speed error, and separation error responses of the ACC vehicles are shown in Figures 10(a)-(c), respectively. The simulation results demonstrate that ACC02 has good string stability properties.

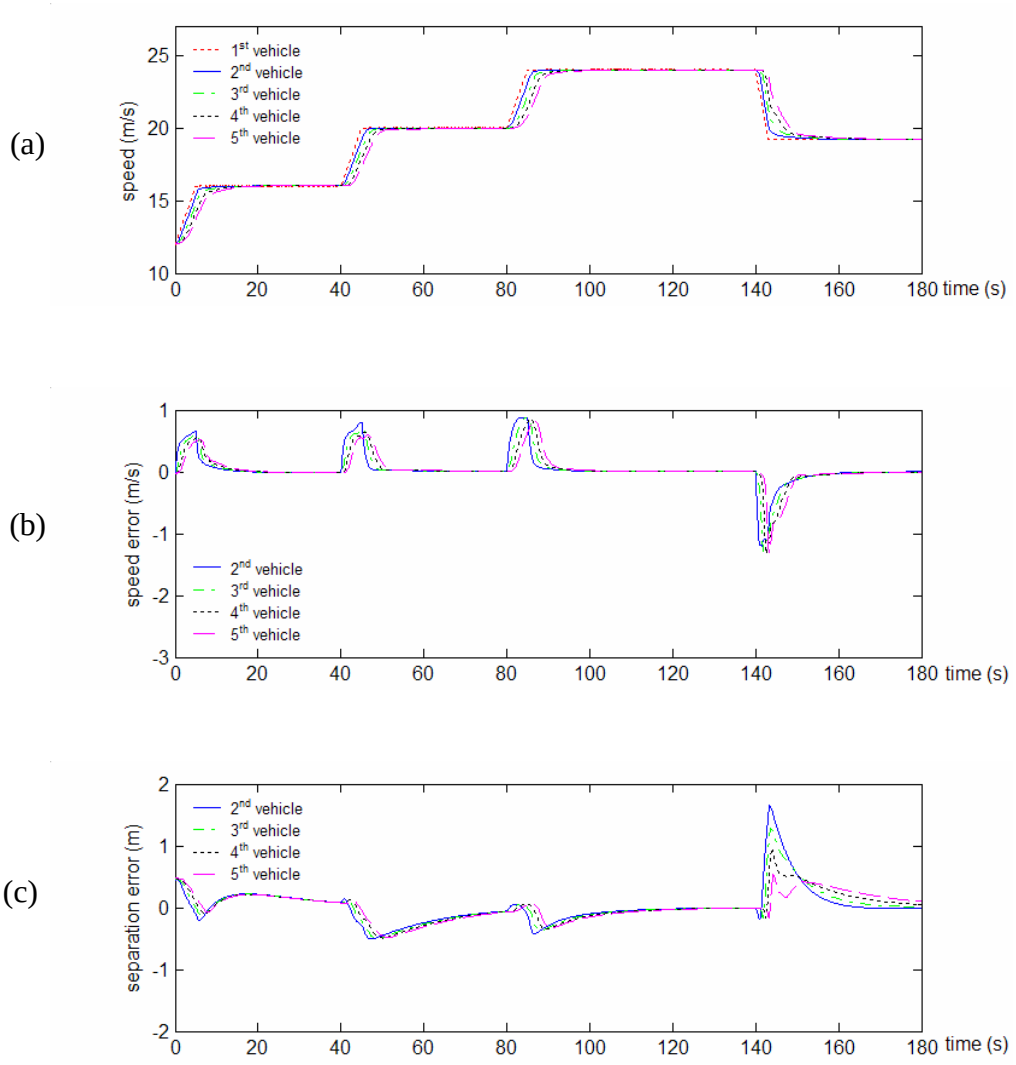

Figure 10. Responses of the following ACC vehicles: (a) speed, (b) speed error and (c) separation error in Simulation C2.

Simulation C3

In this simulation, ten vehicles are simulated and a passenger vehicle equipped with ACC02 is in the second position. The other eight vehicles following after the ACC vehicle are manually driven passenger vehicles simulated with the Pipes' model (2-48). At time zero, all the vehicles have zero speed. From t = 0s to t = 6s, the lead vehicle increases its speed with a constant acceleration 2m/s^2, and then cruises at 12m/s. From t = 50s to t = 56s, the lead vehicle increases its speed with a constant acceleration 2.0m/s^2, and then cruises at 24m/s. The speeds, acceleration, speed error, separation error responses are presented in Figures 11(a)-(d), respectively.

It can be seen that ACC02 provides better transient responses than ACC01. It provides a smoother speed trajectory for the following passenger vehicles which will lead to better fuel economy and emission results. As shown in Figure 11(b), the acceleration is strictly bounded by $a_{\max}$. Since the ACC vehicle responds in a smooth way, the speed and separation errors are temporarily large. At steady state however the control objective is achieved in a smooth manner satisfying all the safety and driver comfort constraints.

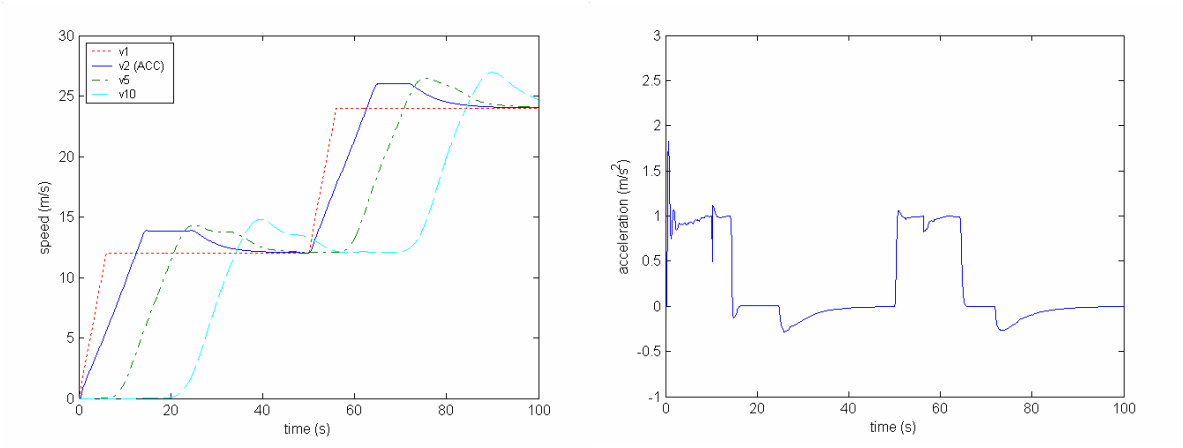

(a) (b)

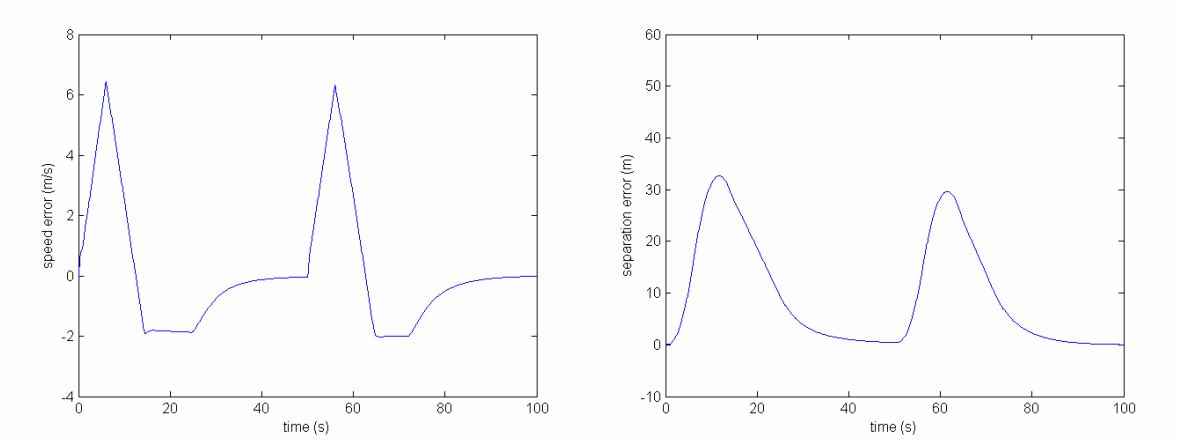

(c) (d)

Figure 11. (a) Speed responses in the vehicle string, and responses of the ACC vehicle: (b) acceleration, (c) speed error and (d) separation error in Simulation C3.

Simulation C4

In this simulation, ten vehicles are simulated and a passenger vehicle equipped with ACC02 is in the second position. The other eight vehicles following the ACC vehicle are manually driven passenger vehicles simulated with the Pipes' model (2-48). At time t = 0s the lead vehicle begins to accelerate from 0m/s with a constant acceleration of 2.0m/s^2 for 6 seconds, and its speed oscillates around 12m/s before settling to the constant speed of 12m/s. At time t = 50second, the lead passenger vehicle accelerates again with 2.0m/s^2 for another 6 seconds and its speed oscillates around 24m/s before settling to a constant speed. The speeds, acceleration, speed error, separation error responses are presented in Figures 12(a)-(d), respectively. The ACC vehicle responds in a smooth way, and the oscillations in the speed of the lead vehicle are not propagated upstream by the ACC vehicle due to the use of (2-57). This demonstrates the ability of the ACC02 to reject disturbances which would otherwise be propagated upstream by most of the existing ACC systems.

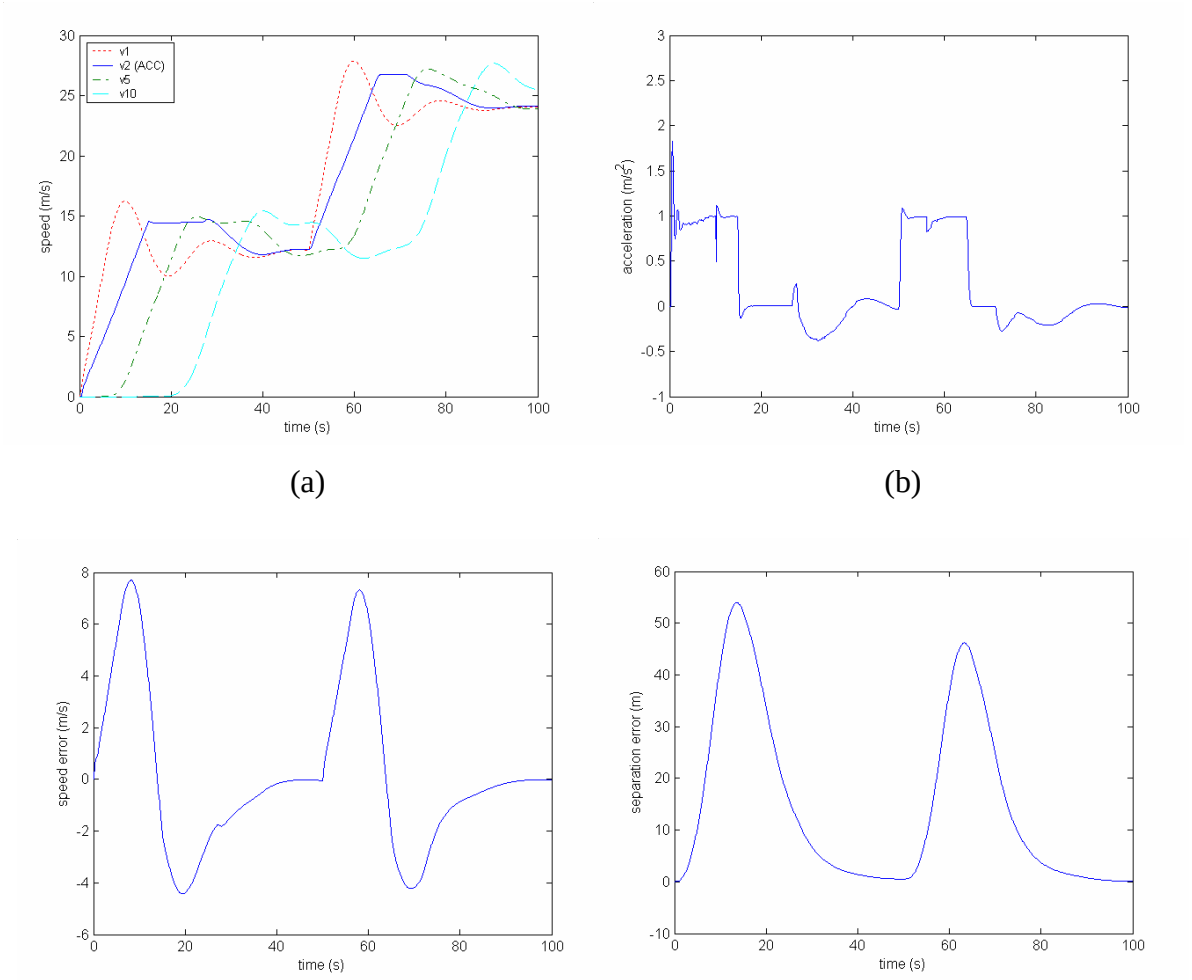

Figure 12. (a) Speed responses in the vehicle string, and responses of the ACC vehicle: (b) acceleration, (c) speed error and (d) separation error in Simulation C4.

3 ENVIRONMENTAL CONSIDERATIONS

It has been demonstrated via extensive simulations and actual experiments that the presence of 10% ACC vehicles in mixed traffic could lower fuel consumption and pollution levels by as much as 8% and 3.8% to 47.3% respectively during certain traffic disturbance scenarios [9]. Our simulation results demonstrate that the ACC system designed in section 2.4 (ACC01) with different time headways provides similar transient responses as the one investigated in [9], and leads to similar fuel consumption and emission results. The work that has been done in [9] won't be repeated here. However, the ACC system designed in section 2.5 (ACC02) can regulate the vehicle speed in a more intelligent way and provide better transient response than ACC01 (see Simulations 3, 4, C3 and C4). In this section, we investigate the impact of ACC02 on mixed traffic, with comparison to ACC01, in terms of emission and fuel consumption using the simulation results presented in sections 2. ACC01 has very similar properties as most existing ACC systems and is a good benchmark to be used in evaluating the performance of the improved and more intelligent ACC which we referred to as ACC02.

In our work, the Comprehensive Modal Emissions Model (CMEM) developed at UC Riverside is used to analyze the vehicle data and calculate the air pollution and fuel consumption [36]. It calculates vehicle emissions and fuel consumption as a function of the vehicle operating mode, i.e. idle, steady state cruise, various levels of acceleration/deceleration, and other variables associated with road and vehicles characters. A simple diagram for the CMEM model is shown in Figure 13. In our simulations, we selected the vehicle category to be 5, which is the most common vehicle type in California: high-mileage, high power-to-weight. The inputs for the CMEM model are vehicle longitudinal speed and acceleration data, while road grade is taken to be zero and no wind gust is considered. Other variables associated with vehicle accessories like air-conditioning are also neglected. The outputs generated by the CMEM models include second-by-second tailpipe emissions of unburned hydrocarbons (HC), oxides of carbon (CO, CO_2), oxides of nitrogen (NO, NO_2, denoted by NO_x) and fuel consumption. More detailed information about the emission model can be found in [36].

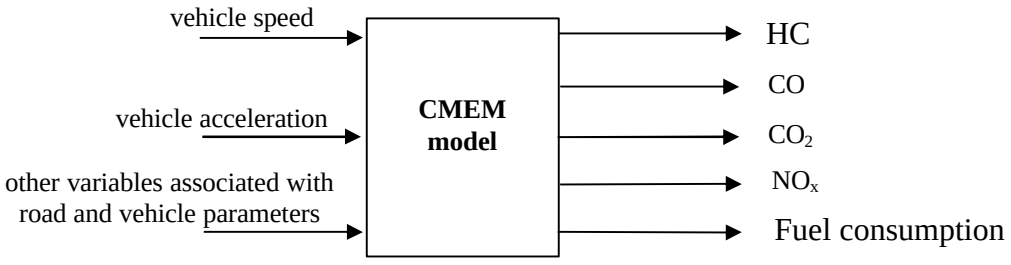

Figure 13. Diagram of the CMEM model

We investigate and compare the behavior of two vehicle strings, each containing ten vehicles. In vehicle string 1, the lead vehicle generates different speed trajectories, the second vehicle is a passenger vehicle equipped with ACC01, and all the other eight vehicles are manually driven passenger vehicles (modeled using the Pipes' model (2-48)). Vehicle string 2 is the same as vehicle string 1, but its second vehicle is replaced by a passenger vehicle equipped with ACC02. We investigate how vehicles equipped with ACC02, compared to those with ACC01, in terms of travel time, fuel efficiency and emissions calculated using the emission model in [36] and the simulation results in Simulations 3, 4, C3 and C4 presented in section 2. In our study we assume that no lane changes take place despite the creation of possibly large intervehicle spacing during vehicle maneuvers.

Since the simulations results of section 2 demonstrated that the ACC01 and ACC02 have very similar response at low lead acceleration maneuvers, we only consider the following two tests involving high lead vehicle accelerations, in which the ACC01 and ACC02 behave differently.

Test 1: High Acceleration Maneuvers

The purpose of this test is to compare the effects of ACC01 and ACC02 on the behavior of the following eight passenger vehicles when the lead vehicle performs a high acceleration maneuver creating a disturbance that propagates upstream.

At t = 0s, the lead passenger vehicle begins to accelerate from speed 0m/s with a constant acceleration of 2.0m/s^2 for 6 seconds, cruises at a constant speed until t = 50s, accelerates with 2.0m/s^2 for another 6 seconds, and then cruises at a constant speed 24m/s. We calculate the fuel consumption and emissions of each vehicle from the time the lead vehicle begins to accelerate, until the string covers a distance of 1.5km. The travel time is recorded over a distance of 1.5km as this is the distance taken by the vehicles to reach a steady state speed after completing the acceleration maneuver.

Table 2 shows the travel times, fuel consumption and emission data for the nine following passenger vehicles in the two vehicle strings. The percentage numbers in the last column represent the fuel and emission benefits of ACC02 over ACC01. As we can see, the presence of ACC02 will not affect the travel time of the following passenger vehicles. However, it has better disturbance rejection properties presenting a smoother speed response to be tracked by the following passenger vehicles in the presence of a wide class of high acceleration maneuvers performed by the lead vehicle. This property of ACC02 accounts for the fuel and emission benefits shown in Table 2.

Test 2: High Acceleration Maneuvers with Oscillations

The purpose of this test is to compare the impacts of ACC01 and ACC02 on the behavior of the following 8 passenger vehicles when the lead vehicle performs a high acceleration oscillatory maneuver creating a disturbance that propagates upstream.

At time t = 0s, the lead passenger vehicle begins to accelerate from 0m/s with a constant acceleration of 2.0m/s^2 for 6 seconds, and its speed oscillates around 12m/s before settling to the constant speed of 12m/s. At time t = 50s, the lead passenger vehicle accelerates again with 2.0m/s^2 for another 6 seconds and its speed oscillates around 24m/s before settling to a constant speed. The travel time is recorded over a distance of 1.5km as this is the distance taken by the vehicles to reach a steady state speed after completing the acceleration maneuver.

Table 3 shows the travel time, fuel consumption and emission results for the nine following passenger vehicles in each vehicle string. The travel times of the following passenger vehicles for the two vehicle strings are the same. It follows from Table 3 that the presence of ACC02, compared with ACC01, can significantly improve fuel efficiency and decrease emissions. This is due to the fact that ACC02 is designed to provide smooth response and reject disturbances such as oscillations which do not contribute to travel time and do not affect safety.

String of 10 vehicles	ACC01 in the 2nd position	ACC02 in the 2nd position
Travel Time (sec)	101.7	101.7
Fuel (g)	1327	1095 (17.5%)
CO_2 (g)	3632	3205 (11.8%)
CO (g)	356	164 (53.9%)
HC (g)	5.85	3.02 (48.4%)
NO_x (g)	7.22	4.56 (36.8%)

Table 2. Travel time, fuel consumption and emission data of the 9 passenger vehicles in a string of 10 vehicles for high acceleration maneuvers of the lead vehicle (no cut-ins)

String of 10 vehicles	ACC01 in the 2nd position	ACC02 in the 2nd position
Travel Time (sec)	100.3	100.3
Fuel (g)	1482	1134 (23.5%)
CO_2 (g)	4003	3289 (17.8%)
CO (g)	429	191 (55.5%)
HC (g)	7.13	3.38 (52.6%)
NO_x (g)	8.82	5.10 (42.2%)

Table 3. Travel time, fuel consumption and emission data of the 9 passenger vehicles in a string of 10 vehicles for high acceleration maneuvers with oscillations of the lead vehicle (no cut-ins)

In our approach we assume that the lead vehicle reaches a steady state giving time for the ACC vehicle to close in by using a higher speed leading to a travel time that is not affected by the presence of the ACC vehicle. We can also create scenarios where the travel time will be affected when the ACC vehicle does not speed up to close in with the lead vehicle especially when the lead vehicle accelerates rapidly and stays at the speed limit that the ACC vehicle cannot exceed. In such situations another effect takes place as

the sluggish response of the ACC vehicle creates large intervehicle gaps inviting vehicles from neighboring lanes to cut in front of the ACC vehicle. This effect has been studied in [37] and is not considered here.

4 TRAFFIC FLOW CONSIDERATIONS

In this section we investigate the effect of ACC vehicles on traffic flow characteristics in mixed traffic on the macroscopic level using the fundamental flow-density diagram. A fundamental flow-density diagram defines the steady-state relation between the traffic flow rate q and the traffic density k. The precise definitions of these two traffic variables and the means of measuring them are explained in [38]. We outline flow-density diagrams for 100% manual/ACC vehicles traffic, and discuss the flow-density curves of the mixed traffic. The manual traffic flow-density curve discussed in this report is constructed using the linear relationship between speed and density hypothesized by Greenshields [22]. There are two time headways considered for ACC vehicles: one is the constant time headway, and the other is a variable time headway modified based on the Greenshields relationship, i.e., the time headway h_a given as

$$h_a = \frac{r}{k_{jam}\left(v_{free} - v\right)} \tag{4-1}$$

where r is a positive scale constant. Different values may be chosen for r based on the safety or traffic flow concerns.

4.1 Manual Traffic

In constructing the fundamental flow-density diagram for the 100% manual vehicles traffic, we consider the hypothesis in [22] that

$$v = \left(1 - \frac{k}{k_{jam}}\right) v_{free} \tag{4-2}$$

where v is the vehicles' mean speed (or traffic flow speed), v_{free} and k_{jam} are the same terms as those in (2-10) and (4-1). The density corresponding to the jam condition, k_{jam}, is equal to $1/L$ where L is the average spacing occupied by one vehicle when the traffic flow speed is zero. In the following analysis, L incorporates safety spacing at low speeds and is larger than the average length of a vehicle. The Greenshields relationship implies that the average time headway used by human drivers, h_m, is given as

$$h_m = \frac{L}{v_{free} - v} \tag{4-3}$$

(4-3) indicates that human drivers use smaller time headways for lower speeds, or equivalently, higher traffic density.

The traffic flow rate q at steady state measures the number of vehicles moving in a specified direction on the road per unit time and is given by

$$q = kv \tag{4-4}$$

With (4-3), the manual traffic flow-density relationship at steady state is given by

$$q = k\left(1 - \frac{k}{k_{jam}}\right)v_f \tag{4-5}$$

The fundamental q-k diagram labeled as "100% manual" in Figure 14 is generated using (4-5). It follows from (4-5) that the traffic flow rate achieves its maximum value $q_{mm} = \frac{k_{jam} v_{free}}{4}$ at the critical density $k_{cm} = \frac{k_{jam}}{2}$.

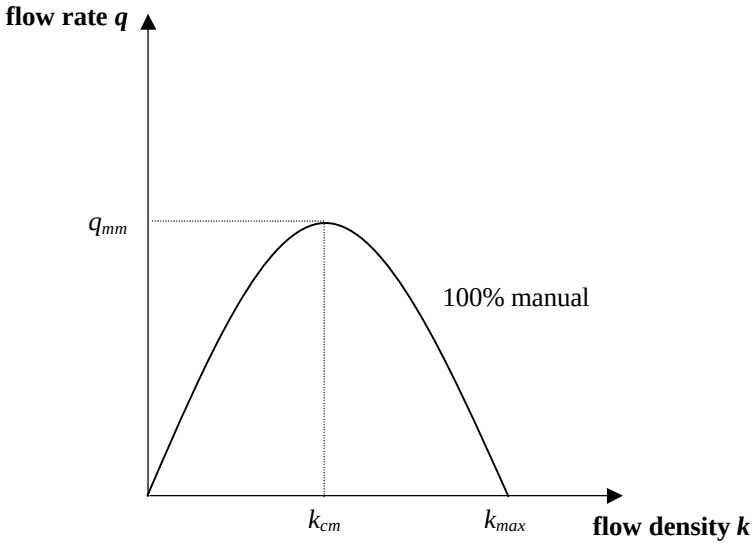

Figure 14. Fundamental flow-density diagram of the manual traffic

If the traffic is dense enough to be viewed as a fluid, then from the conversation of mass equation, we have

$$\frac{\partial k}{\partial t} + \frac{\partial q}{\partial x} = 0 \tag{4-6}$$

Further assuming that the human driver or the ACC system can adjust the vehicle's speed instantaneously to the steady state value based on the current traffic density, we can treat q as a function that depends only on k, and (4-6) can be rewritten as [39]

$$\frac{\partial k}{\partial t} + c\frac{\partial k}{\partial x} = 0 \tag{4-7}$$

where

$$c = \frac{dq}{dk} = v + k\frac{dv}{dk} \tag{4-8}$$

When the traffic density on any road section is close to a constant k_0, c can be approximated as a constant equal to $v(k_0) + k_0 \left.\frac{dv}{dk}\right|_{k=k_0}$, which can be interpreted as the slope of the tangent to the q-k curve at $k=k_0$. When c is a constant, the solution of (4-9) is a traveling wave [39]

$$k(x,t) = F(x - ct) \tag{4-9}$$

where F is an arbitrary differentiable function. If v is a non-increasing function of k, which is true in practice, we can see that $c \le v$ always holds. This means the traveling wave always propagates backwards relative to the traffic flow. If $c > 0$, then any density disturbance propagates as a forward traveling wave. If $c < 0$, then the density disturbance propagates as a backward traveling wave, which indicates that any density disturbance is traveling upstream in the space without any attenuation. Using the flow-density relationship of manual traffic described by (4-5), it can be shown that

$$c = v_f\left(1 - \frac{2k}{k_{jam}}\right) = 2v - v_f \tag{4-10}$$

It follows that c is a strictly decreasing function of k and

$$\begin{cases} c \ge 0, & \text{if } k \in [0,\, k_{cm}] \\ c < 0, & \text{if } k \in (k_{cm},\, k_{jam}] \end{cases} \tag{4-11}$$

In the 100% manual traffic, the q-k curve has a stationary point that corresponds to a critical density k_{cm} that gives the maximum traffic flow rate q_{mm} or the capacity on that section of the road. The point (q_{mm}, k_{cm}) has been empirically observed to be unstable, i.e. it leads to a breakdown in traffic flow [33]. When such traffic flow conditions exist the traffic flow rate and the average speed decrease as the traffic density increases, and the operating point moves towards the jam density k_{jam} on the q-k curve. This observation is explained in [40]. As capacity is approached, the flow tends to become unstable as the number of available gaps reduces. Traffic flow at capacity means that there are no usable gaps left. A disturbance in such a condition due to lane changing or vehicle merging is not “effectively damped” or “dissipated”. As indicated by (4-9) and

(4-11), any disturbance propagates upstream without attenuation. This leads to a breakdown in traffic flow and "formation of upstream queues".

4.2 Impact of ACC Vehicles

While the behavior of human drivers is random and at best we can develop a manual traffic flow-density model that is qualitatively valid, the response of ACC vehicles is more deterministic due to the use of a specific spacing policy. For simplicity we assume that all ACC vehicles have the same length L and use the same spacing policy.

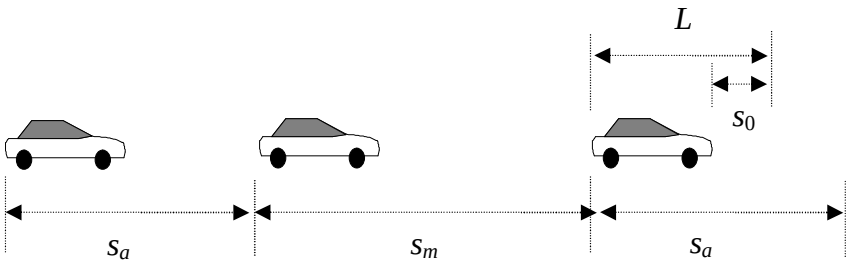

Figure 15. Mixed traffic with ACC and manually driven vehicles.

Consider the mixed traffic flow shown in Figure 15, where s_a and s_m are the average intervehicle spacing used by ACC and manual vehicles, respectively. Note, the safety distance at the congestion conditions, s_0, has been incorporated in L. The average intervehicle spacing at steady state, $\bar{s}$, is given by

$$\bar{s} = ps_a(v) + (1-p)s_m(v) \tag{4-12}$$

where p is the penetration of ACC vehicles. In the following analysis, we consider p to be a positive number. The average traffic density, k_{mix}, is given by

$$k_{mix} = \frac{1}{\bar{s}} = \frac{1}{ps_a + (1-p)s_m} \tag{4-13}$$

(4-13) can be rewritten as

$$q_{mix}(v) = \frac{1}{\frac{p}{q_a(v)} + \frac{1-p}{q_m(v)}} \tag{4-14}$$

where $q_{mix}(v)$, $q_a(v)$, and $q_m(v)$ are the flow rates at speed v for the mixed, ACC, and manual traffic, respectively. In the following analysis, we will always use k, instead of k_{mix}, to represent the traffic flow density of the mixed traffic. We also use the notations k_c

and q_m as the critical density and the maximum flow rate of the mixed traffic, respectively.

4.2.1 Constant Time Headway

In this subsection, we consider the impact of ACC systems which employ constant time headway policy. Consider the 100% ACC traffic case. When the traffic density is low, we can assume no vehicle interaction and all the ACC vehicles operate at the free speed v_{free}. As the traffic density increases, and reaches the critical density k_{ca}, given by

$$k_{ca} = \frac{1}{h_a v_{free} + L} \tag{4-15}$$

where h_a is the average time headway, the ACC vehicles begin to interact with each other. The total spacing, s, occupied by an ACC vehicle using constant time headway h_a at a speed v is given by

$$s = h_a v + L \tag{4-16}$$

Note that the safe distance term s_0 in the spacing policy (2-6) has been incorporated into L. The fundamental flow-density diagram for the traffic with 100% ACC vehicles is given by

$$q = \begin{cases} k v_{free} & 0 \le k \le k_{ca} \\ (1 - kL)/h_a & k_{ca} < k \le k_{jam} \end{cases} \tag{4-17}$$

Equation (4-17) does not capture effects that are due to individual vehicle responses but describes the average steady state traffic flow characteristics. The relationship described by (4-17) is graphically viewed in Figure 16. It follows from (4-17) that the traffic flow rate achieves its maximum value $q_{ma} = \dfrac{v_{free}}{h_a v_{free} + L}$ at the critical density k_{ca}.

For the ACC traffic described by (4-17), it follows that

$$c = \begin{cases} v_{free}, & \text{if } k \in [0, k_{ca}] \\ -\dfrac{L}{h_a}, & \text{if } k \in (k_{ca}, k_{jam}] \end{cases} \tag{4-18}$$

where k_{ca} is the critical density given in (4-15). From (4-18), it follows that the speed of the traveling wave is the same as the average speed of all the ACC vehicles when the traffic density is lower than k_{ca}. When the traffic density is higher than k_{ca}, any disturbance in the traffic will propagate upstream with a constant speed L/h_a. As we can

see, selecting small h_a increases not only the maximum traffic flow rate but also the traveling speed of traffic disturbances.

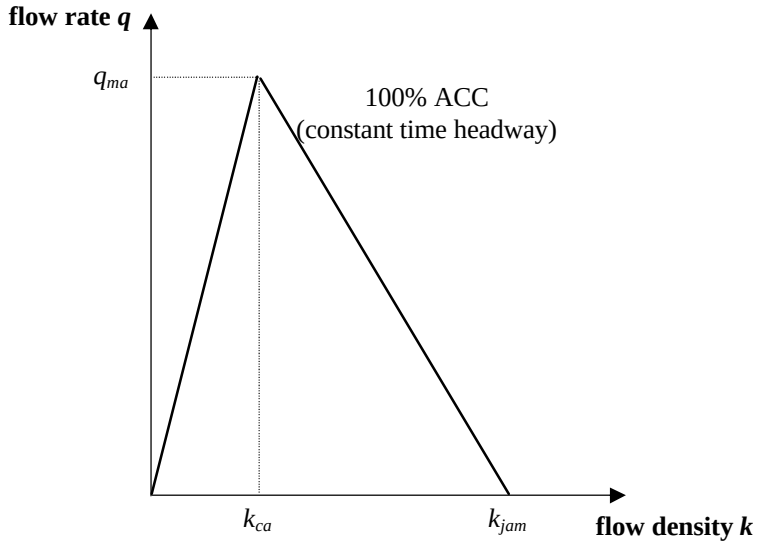

Figure 16. Fundamental flow-density diagram of the ACC traffic (constant time headway).

Using (4-13) and (4-14), it is trivial to show that the traffic density of the mixed traffic is a strictly decreasing function of the flow speed, and that the fundamental flow-density diagram of the mixed traffic must be bounded between those of the 100% ACC traffic and 100% manual traffic. Now we consider the following cases in the mixed traffic:

Case 1: $h_a \geq \dfrac{3L}{v_{free}}$

In this case, k_{ca} is lower than k_{cm} and q_{ma} is lower than or equal to q_{mm}, respectively, as shown in Figure 17. q_{ma} is equal to q_{mm} if and only if $h_a=3L/v_{free}$. Using (4-13) and (4-14), it can be further shown that the critical density, k_c, and the maximum flow rate, q_m, of the mixed traffic are lower than k_{cm} and q_{mm}, respectively. This conclusion indicates that ACC vehicles using large constant time headway (no less than $3L/v_{free}$) will decrease the critical density and the maximum flow rate of the highway traffic, which is undesirable.

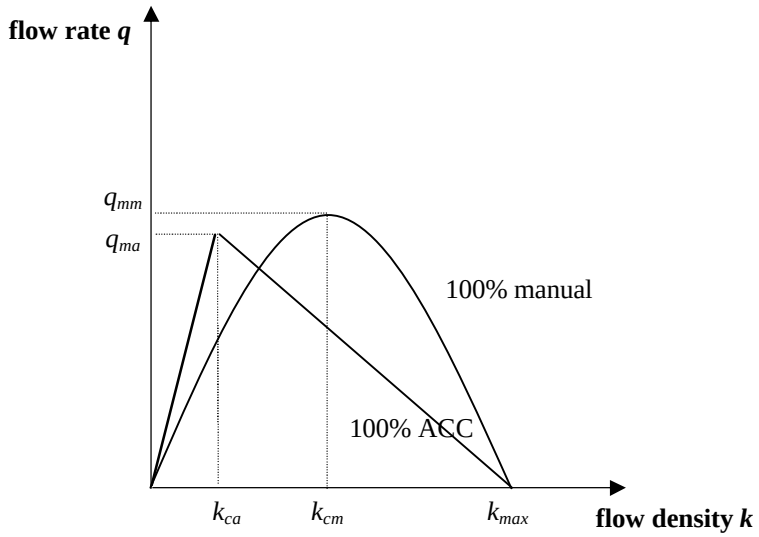

Figure 17. Fundamental flow-density diagrams of the manual traffic and the ACC traffic (constant time headway $h_a \geq 3L/v_{free}$).

Case 2: $\frac{2L}{v_{free}} \leq h_a < \frac{3L}{v_{free}}$

In this case, k_{ca} is lower than k_{cm} but q_{ma} is higher than q_{mm}, as shown in Figure 18. The flow rate of the ACC traffic is not higher than that of the manual traffic at k_{cm}. Using (4-13) and (4-14), it can be further shown that the critical density of the mixed traffic, k_c, is always lower than k_{cm}. However, the relationship between q_m and q_{mm} depends on p, the penetration of the ACC vehicles. q_m is lower than q_{mm} for small p, while q_m is higher than q_{mm} for large p. In this case the presence of ACC vehicles increases the highway capacity when the penetration is high, and it decreases the highway capacity otherwise.

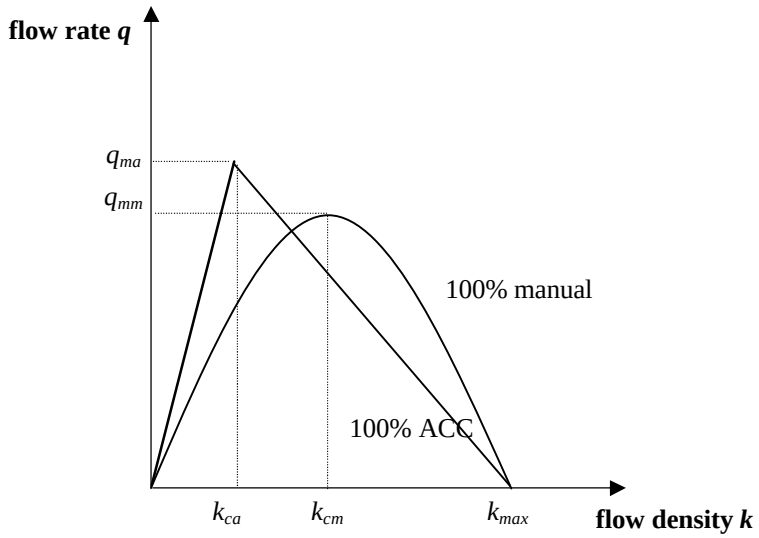

Figure 18. Fundamental flow-density diagrams of the manual traffic and the ACC traffic (constant time headway $2L/v_{free} \le h_a < 3L/v_{free}$).

Case 3: $\frac{L}{v_{free}} < h_a < \frac{2L}{v_{free}}$

In this case, k_{ca} is lower than k_{cm} but q_{ma} is higher than q_{mm}. This case is different from case 2: the flow rate of the ACC traffic at k_{cm} is higher than q_{mm}, as shown in Figure 19. Using (4-13) and (4-14), it can be further shown that q_m is always higher than q_{mm}, which means the presence of ACC vehicles always improves the highway capacity.

Case 4: $h_a \le \frac{L}{v_{free}}$

In this case, h_a is smaller than the average time headways used by human drivers at any density. Its fundamental flow-density curve is not presented here but it can be easily verified that the mixed traffic flow rate is always higher than the manual traffic flow rate. Though it sounds to be an interesting case, using such small time headway is not desirable due to safety considerations.

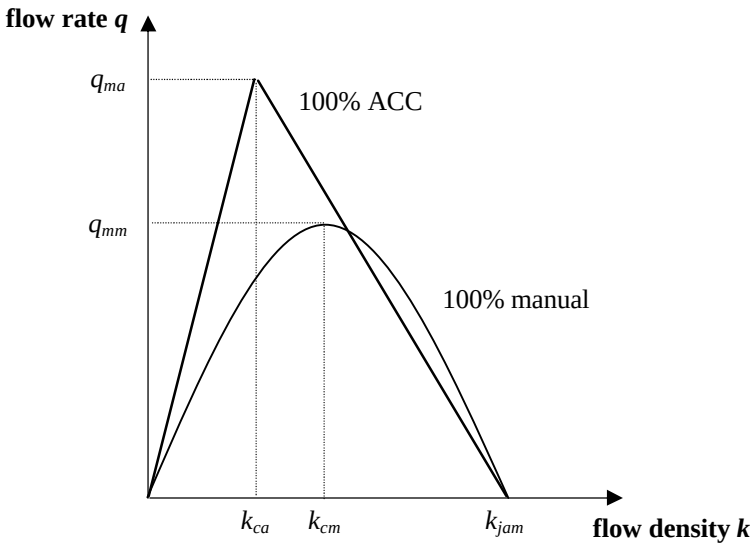

Figure 19. Fundamental flow-density diagrams of the manual traffic and the ACC traffic (constant time headway $L/v_{free}<h_a<2L/v_{free}$).

Now we can have a look at the simulation studies conducted in [21]. It was shown in [21] that using the variable time headway based on the Greenshields relationship can lead to better traffic performance than using the constant time headway. The simulation parameters used in [21] are: v_{free}=36m/s, L=10m (or k_{jam}=100veh/km), and h_a=1s. This situation falls into case 1 in our study. It is not surprising to find out that the variable time headway performs better than the constant one around the traffic density k_{cm}, which agrees with simulation results in [21].

4.2.2 Modified Variable Time Headway based on the Greenshields relationship

As described in (4-1), we assume that the variable time headway used by ACC vehicles, h_a, is r times of that used by human drivers on the average. r is a scaled factor that could be adjusted for safety concerns. When r=1, the time headway used by ACC vehicles is the same as that of the manually driven vehicles. In this subsection, we analyze how ACC vehicles with such variable time headways will affect the traffic flow characteristics. In [31], a similar work has been done for heavy trucks.

From (4-13), it can be derived that

$$k = \frac{1}{p_h h_m v + L_c} \tag{4-19}$$

where $p_h = pr + (1-p)$, h_m is given in (4-4), and k and v are the density and speed of the mixed traffic, respectively. With (4-4), it follows that

$$v = \frac{1-Lk}{1-Lk+p_h Lk} v_f = \left(1 - \frac{p_h Lk}{1-Lk+p_h Lk}\right) v_f \tag{4-20}$$

When p=0, (4-20) is the same as (4-3), and the corresponding fundamental flow-density diagram is labeled as the "0% ACC" in Figures 20 and 21. With (4-4) and (4-20), the traffic flow rate q is given by

$$q = \left(1 - \frac{p_h Lk}{1-Lk+p_h Lk}\right) k v_f \tag{4-21}$$

From (4-21), it follows that

$$\frac{dq}{dk} = \frac{(1-Lk)^2 - p_h L^2 k^2}{(1-Lk+p_h Lk)^2} v_f \tag{4-22}$$

and

$$\frac{d^2 q}{dk^2} = -\frac{2p_h L}{(1-Lk+p_h Lk)^3} v_f \tag{4-23}$$

$k \in [0, 1/L]$ indicates $\frac{d^2 q}{dk^2} < 0$. Hence, q is a strictly concave function of k on [0, 1/L], and $c = \frac{dq}{dk}$ is a strictly decreasing function of k on [0, 1/L]. The maximum traffic flow rate, q_m, is achieved at k_c, where q_m and k_c are given as

$$k_c = \frac{1}{\left(1+\sqrt{p_h}\right)L} \tag{4-24a}$$

$$q_m = \frac{v_f}{\left(1+\sqrt{p_h}\right)^2 L} \tag{4-24b}$$

From (4-20), it follows that the speed of the traveling waves, c, is given by

$$c = \frac{dq}{dk} = \frac{(1-Lk)^2 - p_h L^2 k^2}{(1-Lk+p_h Lk)^2} v_f \tag{4-25}$$

With (4-20), (4-25) can be rewritten as

$$c = \frac{v^2}{v_f} - \frac{(v_f - v)^2}{p_h v_f} \tag{4-26}$$

Using the above equations we examine how the presence of ACC vehicles affects the traffic flow characteristics. We consider the following cases:

Case 1: $r = 1$

In this case, the time headway used by ACC vehicles is the same as that used by manually driven vehicles, or equivalently, $p_h = 1$ for all p. This is a trivial case: the presence of ACC vehicles doesn't affect the traffic flow-density diagram.

Case 2: $r < 1$

In this case, the time headway used by ACC vehicles is smaller than that used by manually driven vehicles. Equivalently, $p_h = 1$ if $p = 0$, and $0 < p_h < 1$ otherwise. The fundamental flow-density diagram of the mixed traffic is labeled as "100p% ACC" shown in Figure 20. From (4-24a) and (4-24b), we know that $k_c > k_{cm} = \frac{1}{2L}$ and $q_m > q_{mm} = \frac{v_f}{4L}$ for nonzero p. This indicates the presence of ACC vehicles increases the critical density and traffic throughput since they are using smaller time headway. It is obvious that for two traffic flows at the same speed, the one with 100p% of ACC will have traveling waves propagating upstream faster, based on (4-26). This point can be graphically viewed as in Figure 20: the slope of the tangent at point A_p is smaller (more negative) than that at point A_0. Following the same analysis, we conclude that for two traffic flows, the one with more percentages of ACC vehicles will have higher critical density and maximum flow rate. For two traffic flows at the same speed, the one with more percentages of ACC vehicles will have traveling waves transferring upstream faster.

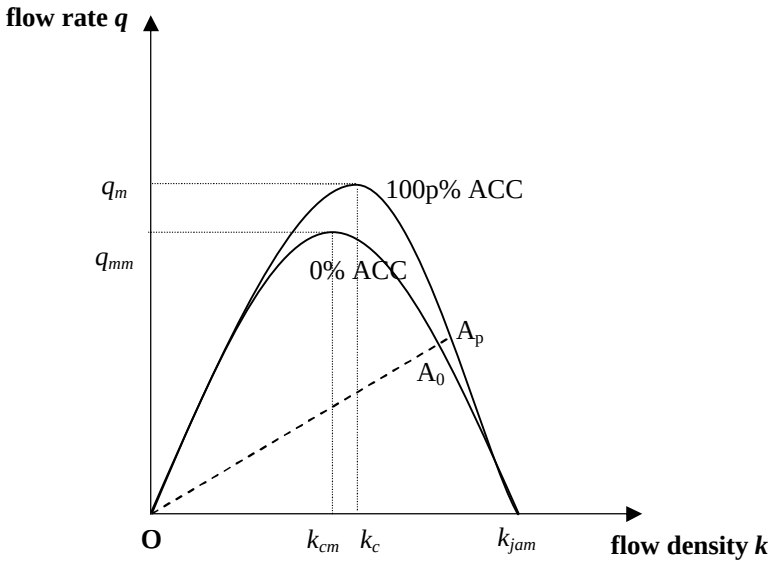

Figure 20. Fundamental flow-density diagrams of the manual traffic and the ACC traffic (variable time headway *r*< 1).

Case 3: $r > 1$

In this case, the time headway used by ACC vehicles is larger than that used by manually driven vehicles. Equivalently, $p_h = 1$ if $p = 0$, and $p_h > 1$ otherwise. The fundamental flow-density diagram is labeled as "100p% ACC" shown in Figure 21. From (4-24a) and (4-24b), we know that $k_c < k_{cm} = \frac{1}{2L}$ and $q_m < q_{mm} = \frac{v_f}{4L}$ for nonzero p. This indicates the presence of ACC vehicles decreases the critical density and traffic throughput since they are using larger time headway than the manually driven vehicles. It is obvious that for two traffic flows at the same speed, the one with 100p% of ACC will have traveling waves propagating upstream slower, based on (4-26). This point can be graphically viewed as in Figure 20: the slope of the tangent at point A_p is larger than that at point A_0. Following the same analysis, we conclude that for two traffic flows, the one with more percentages of ACC vehicles will have lower critical density and maximum flow rate. For two traffic flows at the same speed, the one with more percentages of ACC vehicles will have traveling waves transferring upstream slower.

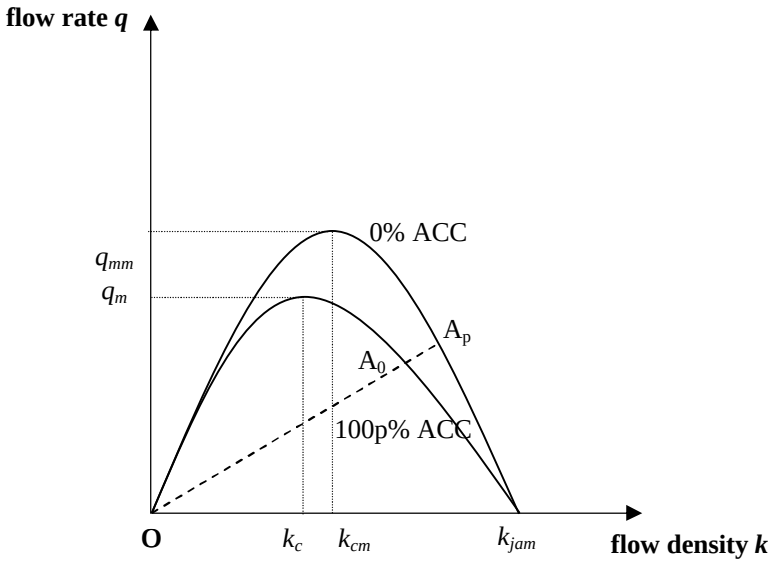

Figure 21. Fundamental flow-density diagrams of the manual traffic and the ACC traffic (variable time headway $r > 1$).

Shock waves are discontinuous waves that occur when traffic on a section of a road is denser downstream than upstream. The waves on the less dense section travel faster than those in the dense section ahead and catch up with them. Then the continuous waves coalesce into a discontinuous wave or a "shock wave" [38]. It can be shown that shock waves travel at a speed, u, given by [38]

$$u = \frac{q_2 - q_1}{k_2 - k_1} \tag{4-27}$$

where (q_1, k_1) and (q_2, k_2) are the traffic flow rates and traffic densities on the two sections, respectively. In the fundamental diagram, this is given by the slope of the chord connecting the two points that represent conditions ahead and behind the shock wave at a and b, respectively (see Figure 22). In this report, we use (4-21) and (4-27) to analyze shock waves. Suppose the traffic speeds ahead and after the shock wave are v_1 and v_2, respectively. The speed of shock waves given by (4-27) is

$$u = v_{free} + \frac{(v_{free} - v_2)^2 v_1 - (v_{free} - v_1)^2 v_2}{(v_1 - v_2) v_{free}} - \frac{(v_{free} - v_2)(v_{free} - v_1)}{v_{free}} \cdot \frac{1}{p_h} \tag{4-28}$$

Given p_h, we can estimate how the presence of ACC vehicles affects the shock waves.

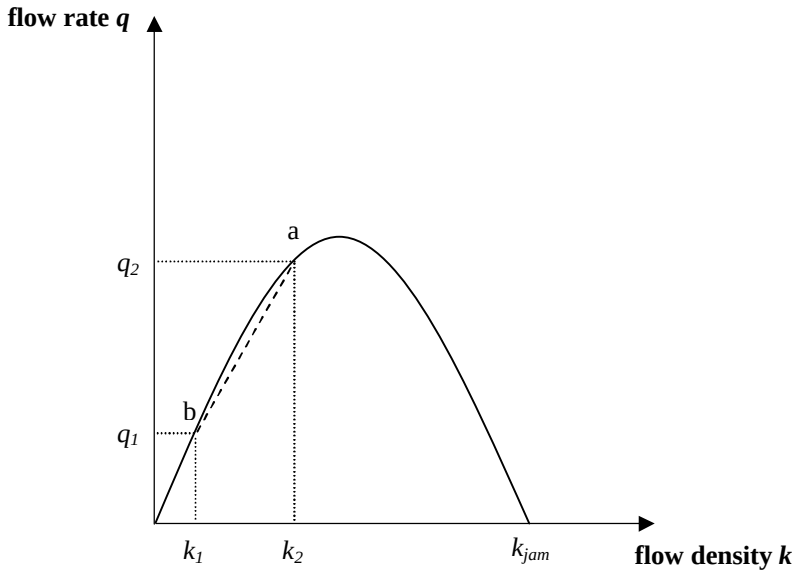

Figure 22. Illustration of shock wave in transportation traffic.

Case 1: $r = 1$

In this trial case, the presence of ACC vehicles doesn't affect the shock waves.

Case 2: $r < 1$

$p_h = 1$ if $p = 0$, and $0 < p_h < 1$ otherwise. This indicates the shock waves are propagated upstream faster in the case of mixed traffic with ACC vehicles.

Case 3: $r > 1$

$p_h = 1$ if $p = 0$, and $p_h > 1$ otherwise. This indicates the shock waves are propagated upstream slower in mixed traffic with ACC vehicles.

In this mixed traffic, if ACC vehicles use the time headway in (4-1) smaller than manually driven vehicles, then the critical density and the maximum traffic flow rate get improved. Hence it is desired to choose r as small as possible. However, the time headway cannot be chosen arbitrarily small due to safety constraints. In addition the use of smaller r leads to a faster propagation of traffic disturbances or shock waves to their dissipation regions.

5 CONCLUSIONS

In this project, we design two ACC systems, referred to as ACC01 and ACC02 that can be implemented with a general variable time headway that includes those proposed in the literature as well as new ones. The ACC systems are developed based on a simplified longitudinal vehicle model and have been proven to be able to guarantee global stability. Simulations are conducted with a validated nonlinear vehicle model to demonstrate that both ACC systems work in a safe manner and meet the control objectives. The ACC01 has similar properties as the ACC systems proposed in the literature whereas ACC02 is different and is equipped with more intelligence when it comes to disturbance rejection and smooth response. It is observed that under certain conditions the transient response of ACC01 violates the control objective when the preceding vehicle accelerates rapidly. Furthermore, the oscillations in the speed of the preceding vehicle will be propagated back unattenuated by ACC01 even when the separation distance is very large. This is typical of the ACC systems proposed in the literature where in an effort to guarantee tight vehicle following they follow closely oscillatory speed responses of the lead vehicle. ACC02 treats the vehicle following task as a special case of the speed tracking task, and is designed to provide better transient performance by using a nonlinear logic function. As a result the oscillations in the speed response of the preceding vehicle can be efficiently attenuated when the separation distance is large. This special property of ACC02 leads to better fuel economy and emission results than ACC01.

We establish that on the macroscopic level the effect of ACC on traffic flow characteristics depends on the spacing rule used rather than the type of individual control system on board of each vehicle. As a result ACC01 and ACC02 have similar properties on the macroscopic level if both use the same spacing rule. When large constant time headways are used, the presence of ACC vehicles decreases not only the capacity but also the critical density of the traffic flow. We propose and analyze a new variable time headway which is parameterized by a design constant r which is interpreted as the ratio of the time headway used by ACC vehicles versus that of manually driven vehicles. For $r<1$ the presence of ACC vehicles appears to improve the traffic flow characteristics whereas for $r>1$ the traffic flow of mixed traffic becomes unstable at lower traffic densities and at lower traffic flows compared with traffic with no ACC vehicles.

Our study concludes that the ACC02 with the new proposed variable time headway with $r<1$ provides the best performance with respect to vehicle following, environment and traffic flow characteristics. Safety considerations may require r to be not much less than 1 or additional technologies may be used to improve the reaction time of ACC during braking maneuvers. The ACC02 system is also able to receive speed commands from the roadway and respond in a smooth way without any adverse effect on travel time. ACC02 will be used in a continuing project under TO5501 to develop a roadway controller in an integrated roadway/ACC system which can be implemented in today's highway system.

REFERENCES

[1] Ioannou P., *Automated Highway Systems*, Plenum, 1997.

[2] Shladover S., "Review of the State of Development of Advanced Vehicle Control Systems (AVCS)", *Vehicle System Dynamics*, Swets & Zeitlinger, 24, pp. 551-595, 1995.

[3] Bishop J. and W. Stevens, "Results of precursor systems analyses of automated highway systems", Proc. First World Congress on Applications of Transport Telematics and Intelligent Vehicle, 1997.

[4] Zhang W.B., "National Automated Highway System Demonstration: A Platoon System", *IEEE Conference on Intelligent Transportation Systems*, Boston, Massachusetts, Nov. 1997.

[5] Thorpe C., Jochem T. and D. Pomerleau, "The 1997 Automated Highway Free Agent Demonstration", *IEEE Conference on Intelligent Transportation Systems*, Boston, Massachusetts, Nov. 1997.

[6] Bishop Richard, "IVI's Time is Now", *ITS World*, March/April 2001, pp10-11.

[7] Bishop Richard, "Japan's Demo 2000 Wows Attendees", *ITS World*, January/February 2001, pp18-19.

[8] Fancher P., et al, "Fostering Development, Evaluation, and Deployment of Forward Crash Avoidance Systems (FOCUS)", *NHTSA*, Report No. DOT HS 808 437, May 1995.

[9] Bose A. and Ioannou P., "Analysis of Traffic Flow With Mixed Manual and Intelligent Cruise Control Vehicles: Theory and Experiments", California PATH Research Report, UCB-ITS-PRR-2001-13, 2001.

[10] Jolibois S.C. and Kanafani A., "An Assessment of IVHS-APTS Technology Impacts on Energy Consumption and Vehicle Emissions of Transit Bus Fleets", California PATH Research Report, UCB-ITS-PRR-94-19, 1994.

[11] Horan T.A., Hempel L.C., Jordan D.R. and Alm E. A., "ITS and the Environment: Issues and Recommendations for ITS Deployment in California", California PATH Research Report, UCB-ITS-PRR-96-18.

[12] Ioannou P. and Chien C.C. "Autonomous Intelligent Cruise Control", *IEEE Trans. On Vehicular Technology*, vol. 42, no. 4, Nov. 1993.

[13] Broqua F., G. Lerner, V. Mauro, and E. Morello, "Cooperative Driving: Basic Concepts and a First Assessment of Intelligent Cruise Control Strategies", *First Drive Proceedings*, pp. 144-147, 1991.

[14] Minderhood M. and Bovy P.H.L., "Impact of Intelligent Cruise Control in Motorway Capacity", *Transportation Research Record*, No. 1679, 1999, pp. 1-9.

[15] Vandewerf J., Shladover S., Miller M. and Kourjanskaia, "Evaluation of the Effects of Adaptive Cruise Control Systems on Highway Traffic Flow Capacity and Implications for Deployment of Future Automated Systems", *TRB*, paper no. 02-3665, Jan. 2002.

[16] Sony B. and Delorme D., "Human Driver Model for Smart AHS based on Cognitive and Control Approaches", *Proc. of the 10th annual meeting of the Intelligent Transportation Society of America*, Boston, May 2000.

[17] Shladover S.E., "Progressive Deployment Steps Leading Toward an Automated Highway System", *TRB*, Jan. 2000.

[18] B. Van Arem, et al, "An Assessment of the Impact of Autonomous Intelligent Cruise Control", TNO report INRO-VVG, Netherlands, March 1996.

[19] Swaroop D. and Rajagopal K.R. "Intelligent Cruise Control Systems and Traffic Flow Stability", PATH Research Report UCB-ITS-PRR-98-36, Dec. 1998.

[20] Bose A. and Ioannou P., "Evaluation of the Environmental Effects of Intelligent Cruise Control (ICC) Vehicles", *TRB*, ID: 01-2203, January 2001.

[21] Swaroop D. and Huandra R. "Intelligent Cruise Control System Design Based on a Traffic Flow Specification", PATH Research Report, UCB-ITS-PRR-99-5, 1999.

[22] Greenshields B.D., "A study in Highway Capacity", Highway Res. Board Proc, vol. 14, p. 468, 1934.

[23] Yanakiev D., Eyre J. and Kanellakopoulos I., "Analysis, Design and Evaluation of AVCS for Heavy-Duty Vehicles with Actuator Delay: Final report for MOU 240", California PATH Research Report, UCB-ITS-PRR-98-18, 1998.

[24] Broqua F., Lerner G., Mauro V., and Morello E., "Cooperative driving: Basic concepts and a first assessment of 'intelligent cruise control' strategies", *Advanced Telemat-ics in Road Guidance. Proceedings of the DRIVE Conference*, pp. 908-929, Elsevier, February 4-9 1991.

[25] Chang T.-H. and Lai I.-S., "Analysis of characteristics of Mixed Traffic Flow of Autopilot Vehicles and Manual Vehicles", *Transportation Research Part C: Emerging Technologies*, vol. 5c, no. 6, Dec. 1997, pp. 333-348.

[26] Ioannou P. and Xu T., "Throttle and Brake Control", *IVHS Journal*, vol. 1(4), pp. 345-377, 1994.

[27] Palmquist, U, "*Intelligent Cruise Control and Roadside Information*", IEEE Micro, pp.20-28, 1993.

[28] Wang J. and Rajamani R., "Adaptive cruise control system design and its impact on traffic flow," *Proceedings of the American Control Conference*, Anchorage, Alaska, May 2002.

[29] Kanaris A., Ioannou P. and Ho F., "Spacing and Capacity Evaluations for Different AHS Concepts", California PATH Research Report, UCB-ITS-PRR-96-30, 1996.

[30] Fenton R.E., "A Headway Safety Policy for Automated Highway Operations," *IEEE Transactions on Vehicular Technology*, vol. VT-28, pp. 22–28, 1979.

[31] Zhang J. and Ioannou P., "Control of Heavy-Duty Trucks: Environmental and Fuel Economy Considerations", California PATH Research Report, UCB-ITS-PRR-2004-15, 2004.

[32] Swaroop D. and Hedrick J.K., "String Stability of Interconnected Systems", *IEEE Trans. on Automatic Control*, vol. 41, No. 3, pp. 349-357, 1996.

[33] Bose A., Ioannou P., "Mixed Manual/Semi-Automated Traffic: A Macroscopic Analysis", California PATH Research Report, UCB-ITS-PRR-2001-14, 2001.

[34] Ioannou P. and Sun J., *Robust Adaptive Control*, Prentice Hall, 1996.

[35] Pipes L.A., "An Operational Analysis of Traffic Dynamics", *Journal of Applied Physics*, vol. 24, pp. 271-281, 1953.

[36] Barth M.J., et al, "User's Guide: Comprehensive Modal Emissions Model, Version 2.0", University of California, Riverside, 2001.

[37] Ioannou P. and Stefanovic M., "Evaluation of the ACC Vehicles in Mixed Traffic: Lane Change Effects and Sensitivity Analysis", California PATH Research Report, UCB-ITS-PRR-2003-03, 2003.

[38] Lighthill M.J. and Whitham G.B., "On Kinematic Waves II. A Theory of Traffic Flow on Long Crowded Roads", *Proceedings of the Royal Society of London*, Series A 229, pp. 317-345, 1955.

[39] Papageorgiou M., *Applications of Automatic Control Concepts to Traffic Flow Modeling and Control*, Springer, 1983.

[40] 1985 Highway Capacity Manual.